Comparison of Cost-effective Distances for LFAC with HVAC and HVDC in Their Connections for Offshore and Remote Onshore Wind Energy

Xin Xiang, *Member, IEEE*, Shiyuan Fan, Yunjie Gu, *Senior Member, IEEE*, Wenlong Ming, *Member, IEEE*, Jianzhong Wu, *Member, IEEE*, Wuhua Li, *Member, IEEE*, Xiangning He, *Fellow, IEEE*, and Timothy C. Green, *Fellow, IEEE*

***Abstract*—For a cost-effective connection of large-scale long-distance wind energy, a low frequency alternating current (LFAC) transmission scheme (16.7 Hz or 20 Hz) is proposed as an alternative to the conventional high voltage alternating current (HVAC) transmission scheme (50 Hz or 60 Hz) and the recently popular high voltage direct current (HVDC) transmission scheme (0 Hz). The technical feasibility of the LFAC system is demonstrated but the basis for identifying the distance ranges for which LFAC would be preferable to HVAC and HVDC are not established and the dependence of this range on factors, such as power transfer rating, voltage rating and cable/line type, is not investigated. This paper presents an in-depth analysis for the overall cost of LFAC system and then provides an extensive comparison with HVAC and HVDC, to explore the distance ranges over which LFAC is cost-effective over both HVAC and HVDC in connections of offshore and remote onshore wind energy. The results demonstrate that the LFAC system does possess ranges in the intermediate distance for which it is more cost-effective than both HVAC and HVDC, and its overall cost advantage is generally larger in the overhead line (OHL) connection of remote onshore wind energy than the cable connection of offshore wind energy.**

***Index Terms*—Cost-effective ranges, LFAC, overall cost analysis, wind energy.**

NOMENCLATURE

A. Acronyms

C	Overall Cost.
CC	Capital Cost.
CBC	Cable Cost.
CPC	Compensation Cost.
CSC	Current Source Converter.
FFTS	Fractional Frequency Transmission System.
HVAC	High Voltage Alternating Current.
HVDC	High Voltage Direct Current.
LC	Power Losses Cost.
LFAC	Low Frequency Alternating Current.
OHC	Overhead Line Cost.
OHL	Overhead Line.
RC	Route Cost.
RCC	Route Capital Cost.
RLC	Route Power Losses Cost.
RMS	Root Mean Square.
TC	Terminal Cost.
TCC	Terminal Capital Cost.
TLC	Terminal Power Losses Cost.
VSC	Voltage Source Converter.

B. Constants

B_{C}	Base cost for VSC–HVDC offshore platform and plant (25 M£).
B_{T}	Base cost for HVAC offshore platform and plant (5 M£).
E	Energy average price (50 £/MWh).
F	Power factor of HVAC system (1.0).
$f_{\mathrm{T,C}}$	Cost factor of transformer number or converter number per platform (0.2).
QC_{off}	Offshore compensation cost (0.025 M£/Mvar).
QC_{ons}	Onshore compensation cost (0.015 M£/Mvar).
T_{p}	Project time (15 years).
V_{C}	Variable cost for VSC–HVDC offshore platform and plant (0.109 M£/MVA).
V_{T}	Variable cost for HVAC offshore platform and plant (0.045 M£/MVA).
δ_{op}	Operation factor (0.231).
$\vartheta_{\mathrm{offT}}$	Offshore HVAC transformer plant efficiency (99.4%).
$\vartheta_{\mathrm{offC}}$	Offshore VSC–HVDC converter plant (rectifier with transf.) efficiency (98.28%).
$\vartheta_{\mathrm{onsT}}$	Onshore HVAC transformer plant efficiency (99.4%).
$\vartheta_{\mathrm{onsC}}$	Onshore VSC–HVDC converter plant (inverter with transf.) efficiency (98.19%).

Manuscript received December 27, 2020; revised March 2, 2021; accepted April 7, 2021. Date of online publication April 30, 2021; date of current version July 2, 2021. This work was supported by the National Natural Science Foundation of China (51925702, 52107214) and China-UK NSFC-EPSRC Joint Project (52061635101, EP/T021780/1).

X. Xiang, S. Y. Fan, W. H. Li (corresponding author, e-mail: woohualee@zju.edu.cn; ORCID: https://orcid.org/0000-0002-0345-5815) and X. N. He are with the College of Electrical Engineering, Zhejiang University, Hangzhou 310027, China.

Y. J. Gu is with the Department of Electronic and Electrical Engineering, University of Bath, Bath BA2 7AY, UK.

W. L. Ming and J. Z. Wu are with the School of Engineering, Cardiff University, CF24 3AA Cardiff, UK.

T. C. Green is with the Department of Electrical and Electronic Engineering, Imperial College London, London, SW7 2AZ, UK.

DOI: 10.17775/CSEEJPES.2020.07000

$\vartheta_{\text{onsCSC}}$ Onshore CSC–HVDC converter plant (inverter with transf.) efficiency (99.12%).

C. Variables

C Subsea cable shunt capacitance per kilometer (F/km).
c_{C} Subsea cable cost per set including supply and installation (k£/km).
c_{o} Onshore OHL cost per set including supply and installation (k£/km).
f_n Operation frequency (Hz).
I_{ch} Capacitive charging current in subsea cable (kA).
I_{cn} Subsea cable nominal current (kA).
I_{on} Onshore OHL nominal current (kA).
I_{Qoff} Offshore compensation current (kA).
L Onshore OHL series inductance per kilometer (H/km).
l_{c} Subsea cable length (km).
l_{o} Onshore OHL length (km).
n_{C} HVAC transformer number per platform.
n_{T} VSC–HVAC converter number per platform.
nc_{C} Number of subsea cable parallel circuits.
nc_{o} Number of Onshore OHL parallel circuits.
P_{c} Active power transfer capability in subsea cable (MW).
P_{o} Active power transfer capability in onshore OHL (MW).
P_{stl} Stability limit in onshore OHL (MW).
P_{thl} Thermal limit in onshore OHL (MW).
Q_{c} Reactive power produced by capacitive charging current (Mvar).
Q_{off} Offshore compensation power (Mvar).
Q_{ons} Onshore compensation power (Mvar).
r_{C} Subsea cable resistance per kilometer (Ω/km).
r_{o} Onshore OHL resistance per kilometer (Ω/km).
S_{C} Apparent power in subsea cable (MVA).
S_{TT} Power transfer rating (MVA).
V_{cn} Subsea cable nominal voltage (kV).
V_{on} Onshore OHL nominal voltage (kV).
X_{o} Onshore OHL series reactance per kilometre (Ω/km).

I. Introduction

WIND is regarded as one of the most important renewable energy resources throughout the world [1]–[3]. The total penetration of wind generation in some countries has already exceeded 20% of their total capacity [4]. It has also been determined that wind resources are often best installed in offshore or remote onshore areas [5], [6]. For instance, the offshore wind farm generation in Europe is approaching 25 GW as of 2020 and is planned to reach 70 GW by 2030 [7], and the largest wind farm station in the world, which is located in Jiuquan, China (remote onshore area), has already reached 10 GW capacity [8]. These large-scale wind farms are usually far away from the metropolitan load centers, and this fact has prompted a greater effort to advancing cost-effective long-distance transmission technologies in connection with wind energy [9], [10].

High voltage alternating current (HVAC) and high voltage direct current (HVDC) systems, illustrated in Fig. 1 and Fig. 2, have been commercialized for this use in both subsea cable form in connection with offshore wind energy and overhead line (OHL) form in connection with remote onshore wind energy [11]–[14]. The overall cost of a wind energy connection system is usually partitioned into the terminal cost and route cost for analysis and comparison [15]–[18]. A HVAC system has the advantage of relatively inexpensive terminal costs, whereas a HVDC system has an expensive power converter plant at each terminal. The route cost in a HVAC system rises much more sharply with distance than that in a HVDC system because of the different transmission capability limits in the AC and DC use of cables and OHL. Over short distances, a HVAC system is favored for its lower terminal costs but beyond some threshold distance, the advantages of lower route costs favors the HVDC system. The cross-over distance for the overall cost of HVAC and HVDC systems is reported to be in the region of 80 km [19]–[21] for a subsea cable system and 700 km for a remote onshore OHL system [22], [23].

However, the technology choice for HVAC or HVDC on a distance basis is not yet definitive. For example, the very recent practical wind farm projects of Hornsea [24], [25] and Dogger Bank [26], [27] made different choices (Hornsea chose HVAC while Dogger Bank chose HVDC) although they are located in the same area of the North Sea with almost the same power rating. This could raise a general equation whether there exists a third technology choice with cost advantages over both HVAC and HVDC for some distance ranges, which may further lower the wind energy price and increase wind energy penetration in the future.

The low frequency alternating current (LFAC) system [28]–[30], or alternatively, fractional frequency transmission system (FFTS) [31]–[34] was proposed in the 1990 s, and its structure for a wind energy connection is shown in Fig. 3. The operational frequency in a LFAC system is usually set at 16.7 Hz or 20 Hz, which is one third of the standard system frequency (50 Hz or 60 Hz) for HVAC. Because of the lower frequency, although the transformer volume tends to increase,

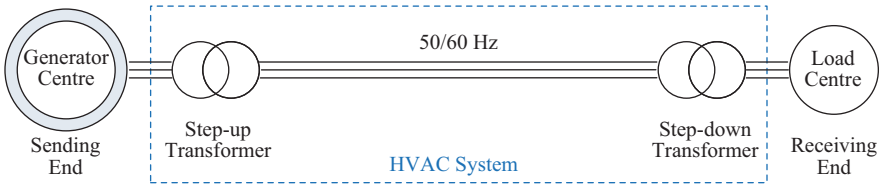

Fig. 1. Structure of HVAC system.

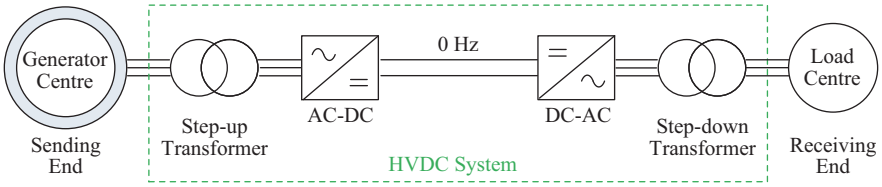

Fig. 2. Structure of HVDC system.

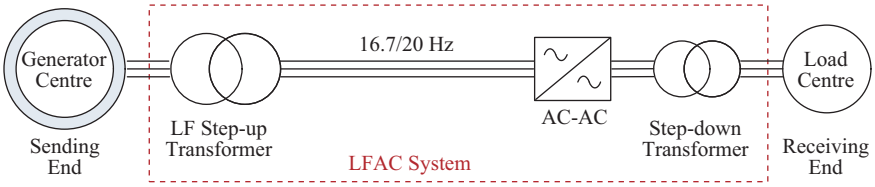

Fig. 3. Structure of LFAC system.

a LFAC system suffers less effects from cable shunt capacitive susceptance or OHL series inductive reactance than a standard HVAC system and so it makes for a more cost-effective use of the cable or OHL. In the case of a wind farms connection, only one AC-AC power converter plant is required as an interface between the LFAC system and the standard electrical network to realize frequency conversion. Therefore, the LFAC system could incur lower terminal costs compared to a HVDC system, and the maintenance costs would also be significantly reduced with the removal of an offshore converter station. Moreover, the voltage stability would be improved since the sensitivity of voltage on reactive power variations is diminished in a LFAC system [35]. Furthermore, a multi-terminal wind energy system could be built relying on LFAC since the protection scheme inherited from the HVAC system has been maturely designed, which is difficult to realize with a HVDC system due to the lack of cost-effective DC breakers. The technical feasibility of a LFAC system has been intensively studied [35]–[38] over the last decade and a laboratory prototype of a LFAC system has also been successfully demonstrated [39], [40]. Cost analysis and comparisons for a LFAC system also received some attention [41]–[43] in recent years but not to the degree needed to properly estimate its cost-effective distance ranges [44]–[46] in connection with wind energy.

It is postulated that a LFAC system would have a lower cost than either HVAC or HVDC systems for some intermediate range of distances straddling the threshold distance between HVAC and HVDC. This is on the basis that a single power converter at one end will provide a lower terminal cost than an HVDC system (but higher than an HVAC system) and better cable or OHL use will give a lower route cost than an HVAC system (but higher than an HVDC system) [46]–[48]. Figure 4 illustrates the overall cost against distance for HVAC, HVDC and three possible cases of LFAC systems. Although all the LFAC cases have terminal costs and unit route costs between those of HVAC and HVDC systems, whether the distance range that exists with the optimal choice of LFAC would also be affected by the power ratings and connection forms has not been determined. In cases 1 and 2, the overall cost of LFAC crosses the overall cost of HVAC before crossing the

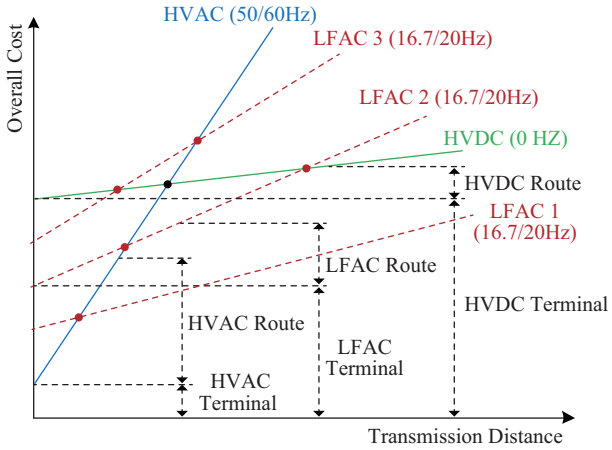

Fig. 4. Three basic possibilities for LFAC overall cost.

overall cost of HVDC and so the LFAC system has a cost-effective range over which it is cheapest. However, in case 3, the overall cost of LFAC first crosses the overall cost of HVDC and then there is no distance for which it is the preferred choice. Therefore, knowing that the terminal costs and unit route costs of the LFAC system lie between those of the HVAC and HVDC systems is not sufficient to establish whether a LFAC scheme has or has not the cost-effective range, let alone identifying the cost-effective distance range for different power ratings with different connection forms. A careful analysis of the overall cost of a LFAC system is required and a thorough comparison with HVAC and HVDC is also needed to bridge this knowledge gap, which can make a good contribution in the future choice of cost-effective technology in connection with large-scale offshore and remote onshore wind energy.

So far, few studies have illustrated the cost estimation for the LFAC based wind energy transmission system. In this paper, an in-depth analysis for the overall cost of a LFAC system is presented and an extensive comparison with HVAC and HVDC is further provided to allow estimation of the cost-effective distance ranges of LFAC over both HVAC and HVDC in connection with offshore and remote onshore wind energy. First, the overall cost of a LFAC system is decomposed

into constituent parts of terminal and route costs and further decomposed into capital and operational costs. Then, detailed analysis of each constituent cost follows with a derivation of equations specific to a LFAC system, and cost parameters are estimated from the most similar equipment used in HVDC and HVAC projects since there is an absence of commercial LFAC projects that can provide cost data. Lastly, the cost estimation process considers different choices of operating voltage and numbers of parallel conductors for each distance in order to meet the specified power transfer at minimum cost and finally provide a fair comparison for these three connection systems. The results demonstrate that a LFAC system does possess a cost-effective distance range over HVAC and HVDC systems in the intermediate distance for both connections of offshore and remote onshore wind energy, and its overall cost advantage is generally larger in the OHL connection of remote onshore wind energy than the cable connection of offshore wind energy.

II. Decomposition of Overall Cost

An all-inclusive analysis of overall cost for a large-scale and long-distance wind energy connection system is complex to conduct in analytical form since many detailed practical factors in the system would need to be taken into consideration and the analysis would become intractable [15], [21]. For a new technology choice, such as a LFAC system, this is complicated by the absence of full-scale demonstration projects which will have resolved some of the implementation details and established design limits. To make the overall cost analysis both feasible and widely applicable, some minor factors in the whole connection system have to be neglected [18], [49], [50] and the cost data of individual items needs to be estimated in broad terms from whatever real practical projects provide a reasonably close data point [51], [52].

It is common to separate out the terminal cost (*TC*) and route cost (*RC*) as the major factors in an estimation of the overall cost (*C*) for a wind energy connection system. The terminal cost is independent of distance while the route cost is a function of distance. Table I lists the cost of each constituent of HVAC, HVDC and LFAC systems under the headings of *TC* and *RC* with reference to Fig. 1–Fig. 3. The descriptions are for an offshore cable connection case with alternative descriptions for a remote onshore OHL connection case given in brackets. The overall cost (*C*) of a wind energy connection system can also be separated into capital cost (*CC*) and the capitalized cost of operational power losses (*LC*). The capital cost is relevantly independent of system operational years while power loss cost is a function of operational years. Thus, the overall cost could be further decomposed as terminal capital cost (*TCC*), terminal power loss cost (*TLC*), route capital cost (*RCC*) and route power loss cost (*RLC*). Fig. 5 shows these two decomposition directions and illustrates the relevant relationships between these constituent costs, and each constituent cost will be discussed and analyzed in detail in the next two sections.

III. Analysis and Estimate of the Cost-effective Range for Offshore Cable Connections

By interpreting each constituent cost in Table I for offshore cable connections in terms of Fig. 5 reveals that *TCC* consists of the offshore platform and plant cost (TCC_{off}) and onshore plant cost (TCC_{ons}), *TLC* consists of offshore plant power loss cost (TLC_{off}) and onshore plant power loss cost (TLC_{ons}); *RCC* consists of the cable cost (*CBC*) and compensation cost (*CPC*), and *RLC* is the subsea cable power loss cost.

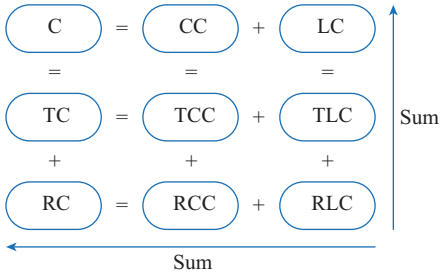

Fig. 5. Decompositions and relationships between constituent costs.

The cost analysis for each constituent in the two established technologies, HVAC and HVDC systems, can draw on the

TABLE I
DECOMPOSITION OF OVERALL COSTS IN HVAC, LFAC AND HVDC SYSTEMS FOR OFFSHORE CABLE CONNECTIONS (WITH VARIATIONS FOR REMOTE ONSHORE OHL CONNECTIONS IN BRACKETS)

System	Terminal cost (*TC*)		Route cost (*RC*)	
	Terminal Capital Cost (*TCC*)	Terminal Power Losses Cost (*TLC*)	Route Capital Cost (*RCC*)	Route Power Losses Cost (*RLC*)
HVAC	Offshore (remote-end) step-up transformer plant and platform (compound). Onshore (load-end) step-down transformer plant and compound.	Cables (or OHL) and compensation.	Offshore (remote-end) transformer plant power losses. Onshore (load-end) transformer plant power losses.	Cables (or OHL) power losses.
HVDC	Offshore (remote-end) converter plant and platform (compound) including valves, transformers and filters. Onshore (load-end) converter plant including valves, transformers and filters.	Cables (or OHL).	Offshore (remote-end) AC-DC converter plant power losses. Onshore (load-end) DC-AC converter plant power losses.	Cables (or OHL) power losses.
LFAC	Offshore (remote-end) LF step-up transformer plant and platform (compound). Onshore (load-end) AC-AC converter plant including valves, transformers and filters.	Cables (or OHL) and compensation.	Offshore (remote-end) LF transformer plant power losses. Onshore (load-end) AC-AC converter plant power losses.	Cables (or OHL) power losses.

published estimation methods and practical cost data. This also serves as an important starting point for the analysis and estimation for the LFAC system. It should be noted that voltage-source-converter HVDC (VSC–HVDC) is the preferred DC option in connection with offshore wind energy so that an isolated AC grid can be formed for the wind turbines.

A. Cost Analysis and Estimate in HVAC and VSC–HVDC Systems

Examining cost data obtained from commercial projects shows that the terminal capital cost for HVAC and VSC–HVDC systems can be approximately estimated by the empirical formula as in (1)–(4) [52]–[56]. For ease of reference, the descriptions for all the variables and relatively assumed values in this paper have been summarized in the Nomenclature section and all the variables will also be described after the specific equation for clarification.

$$TCC_{\text{offHVAC}} = B_{\text{T}} + [1 + f_{\text{T}} \cdot (n_{\text{T}} - 2)] \cdot V_{\text{T}} \cdot S_{\text{TT}} \tag{1}$$

$$TCC_{\text{onsHVAC}} = 0.02621{S_{\text{TT}}}^{0.7513} \tag{2}$$

$$TCC_{\text{offVSCHVDC}} = B_{\text{C}} + [1 + f_{\text{C}} \cdot (n_{\text{C}} - 2)] \cdot V_{\text{C}} \cdot S_{\text{TT}} \tag{3}$$

$$TCC_{\text{onsVSCHVDC}} = 0.08148 S_{\text{TT}} \tag{4}$$

where B_{T} and B_{C} are the base costs for HVAC and VSC–HVDC offshore platform and plant, V_{T} and V_{C} are the variable costs for HVAC and VSC–HVDC offshore platform and plant, n_{T} and n_{C} are the HVAC transformer number and VSC–HVDC converter number per platform, f_{T} and f_{C} are the cost factors for transformer number and converter number per platform, S_{TT} is the transfer power rating.

The capitalized cost of power loss is an accumulated value over an operational time and dependent on an energy price. The power loss cost of the offshore plant and onshore plant for HVAC and HVDC systems are calculated by (5)–(8) respectively [57]–[61].

$$TLC_{\text{offHVAC}} = S_{\text{TT}} \cdot F \cdot (1 - \vartheta_{\text{offT}}) \cdot T_{\text{p}} \cdot \delta_{\text{op}} \cdot E \tag{5}$$

$$TLC_{\text{onHVAC}} = S_{\text{TT}} \cdot F \cdot \vartheta_{\text{offT}} \cdot \vartheta_{\text{CHVAC}} \cdot (1 - \vartheta_{\text{onsT}}) \cdot T_{\text{p}} \cdot \delta_{\text{op}} \tag{6}$$

$$TLC_{\text{offVSCHVDC}} = S_{\text{TT}} \cdot F \cdot (1 - \vartheta_{\text{offC}}) \cdot T_{\text{p}} \cdot \delta_{\text{op}} \cdot E \tag{7}$$

$$TLC_{\text{onsVSCHVDC}} = S_{\text{TT}} \cdot F \cdot \vartheta_{\text{offC}} \cdot \vartheta_{\text{CVSCHVDC}} \cdot (1 - \vartheta_{\text{onsC}}) \cdot T_{\text{p}} \cdot \delta_{\text{op}} \cdot E \tag{8}$$

where F is the power factor for transmission, ϑ_{offT} and ϑ_{onsT} are the efficiencies of an offshore and onshore HVAC transformer plant, ϑ_{offC} and ϑ_{onsC} are the efficiencies of an offshore VSC–HVDC converter plant (rectifier with transformer) and onshore VSC–HVDC converter plant (inverter with transformer), ϑ_{CHVAC} and $\vartheta_{\text{CVSCHVDC}}$ are the efficiencies of HVAC and VSC–HVDC cables, T_{op} is the project time, δ_{op} is the operational factor and E is the energy average price.

Combining (1), (2), (5), (6) and (3), (4), (7), (8) with the assumption values listed in the Nomenclature, the terminal cost of the HVAC and VSC–HVDC systems are estimated as (9) and (10) respectively.

$$\begin{aligned} TC_{\text{HVAC}} &= TCC_{\text{HVAC}} + TLC_{\text{HVAC}} = TCC_{\text{offHVAC}} + \\ &\quad TCC_{\text{onsHVAC}} + TLC_{\text{offHVAC}} + TLC_{\text{onsHVAC}} \\ &= 5 + 0.045 S_{\text{TT}} + 0.02621 {S_{\text{TT}}}^{0.7513} + \\ &\quad 0.00911 S_{\text{TT}} + 0.00906 S_{\text{TT}} \cdot \vartheta_{\text{CHVAC}} \end{aligned} \tag{9}$$

$$\begin{aligned} TC_{\text{VSCHVDC}} &= TCC_{\text{VSCHVDC}} + TLC_{\text{VSCHVDC}} \\ &= TCC_{\text{offVSCHVDC}} + TCC_{\text{onsVSCHVDC}} + \\ &\quad TLC_{\text{offVSCHVDC}} + TLC_{\text{onsVSCHVDC}} \\ &= 25 + 0.11 S_{\text{TT}} + 0.08148 S_{\text{TT}} + 0.02610 S_{\text{TT}} + \\ &\quad 0.02701 S_{\text{TT}} \cdot \vartheta_{\text{CVSCHVDC}} \end{aligned} \tag{10}$$

To estimate the cable cost and compensation cost in a standard HVAC system, the cable transmission capability needs to first be analyzed. Shunt capacitive susceptance is the key parameter limiting active power transfer in a subsea cable, and the reactive power produced by capacitive charging current is expressed as (11).

$$Q_{\text{c}} = 3\left(\frac{V_{\text{cn}}}{\sqrt{3}}\right)^2 \cdot 2\pi f_n \cdot C \cdot l_{\text{c}} = {V_{\text{cn}}}^2 \cdot 2\pi f_n \cdot C \cdot l_{\text{c}} \tag{11}$$

where Q_{c} is the reactive power, V_{cn} is the subsea cable nominal voltage, f_n is the operational frequency, C is the subsea cable shunt capacitance per kilometre and l_{c} is the subsea cable length.

Splitting the reactive power compensation evenly between the two ends of the subsea cable makes available most of the capacity for active power use [21], [51], [62], [63]. On this basis, the cable transmission capability is given by (12), and the compensation cost in the HVAC system can be estimated by (13). With the distance increasing, the cable transmission capability in the HVAC system will decrease and the required compensation power and compensation cost will increase.

$$\begin{aligned} P_{\text{c}} &= \sqrt{{S_{\text{c}}}^2 - {Q_{\text{off}}}^2} = \sqrt{{S_{\text{c}}}^2 - \left(\frac{Q_{\text{c}}}{2}\right)^2} \\ &= \sqrt{\left(\sqrt{3} V_{\text{cn}} I_{\text{cn}}\right)^2 - \frac{1}{4}\left({V_{\text{cn}}}^2 \cdot 2\pi f_n \cdot C \cdot l_{\text{c}}\right)^2} \end{aligned} \tag{12}$$

$$\begin{aligned} CPC_{\text{HVAC}} &= QC_{\text{off}} \cdot Q_{\text{offHVAC}} + QC_{\text{ons}} \cdot Q_{\text{onsHVAC}} \\ &= QC_{\text{off}} \cdot \frac{Q_{\text{cHVAC}}}{2} + QC_{\text{ons}} \cdot \frac{Q_{\text{cHVAC}}}{2} \\ &= \frac{QC_{\text{off}} + QC_{\text{ons}}}{2} \cdot {V_{\text{cn}}}^2 \cdot 2\pi f_n \cdot C \cdot l_{\text{c}} \end{aligned} \tag{13}$$

where P_{c} is the active power transfer capability in the subsea cable, S_{c} is the apparent power in the subsea cable, Q_{off} is the offshore compensation power, I_{cn} is the subsea cable nominal current, QC_{off} and QC_{ons} are the offshore and onshore compensation costs, Q_{off} and Q_{ons} are the offshore and onshore compensation powers.

The parameters of the common cables for a HVAC system are listed in Appendix Table I. The capital costs and power loss costs of HVAC cables are calculated by (14) and (15) respectively, and its efficiency in transmission is expressed in (16).

$$CBC_{\text{HVAC}} = c_{\text{c}} \cdot l_{\text{c}} \cdot nc_{\text{c}} \tag{14}$$

$$\begin{aligned} RLC_{\text{HVAC}} &= 3\left(\frac{S_{\text{TT}} \cdot F \cdot \vartheta_{\text{offT}}}{nc_{\text{c}} \cdot 3\frac{V_{\text{cn}}}{\sqrt{3}}}\right)^2 r_{\text{c}} \cdot l_{\text{c}} \cdot nc_{\text{c}} \cdot T_{\text{p}} \delta_{\text{op}} E \\ &= \left(\frac{S_{\text{TT}} \cdot F \cdot \vartheta_{\text{offT}}}{V_{\text{cn}}}\right)^2 \frac{r_{\text{c}} \cdot l_{\text{c}}}{nc_{\text{c}}} \cdot T_{\text{p}} \delta_{\text{op}} E \end{aligned} \tag{15}$$

$$\vartheta_{\text{CHVAC}} = \frac{S_{\text{TT}} \cdot F \cdot \vartheta_{\text{offT}} - \left(\frac{S_{\text{TT}} \cdot F \cdot \vartheta_{\text{offT}}}{V_{\text{cn}}}\right)^2 \frac{r_{\text{c}} \cdot l_{\text{c}}}{nc_{\text{c}}}}{S_{\text{TT}} \cdot F \cdot \vartheta_{\text{offT}}} = 1 - \frac{S_{\text{TT}} \cdot F \cdot \vartheta_{\text{offT}}}{{V_{\text{cn}}}^2} \cdot \frac{r_{\text{c}} \cdot l_{\text{c}}}{nc_{\text{c}}} \quad (16)$$

where c_{c} is the subsea cable cost per set including supply and installation, nc_{c} is the number of subsea cable parallel circuits, r_{c} is the subsea cable resistance per kilometer.

A VSC–HVDC system has an advantage in active power transfer over HVAC since a DC system can utilize the peak value of voltage continuously whereas the root-mean-square (RMS) value of voltage that sets the AC power is a factor of $\sqrt{2}$ less than the peak value. Moreover, there is no capacitive shunt current in the DC cable transmission, which enlarges the advantages in active power transfer for smaller cable cost and also avoids the compensation cost.

The parameters of the common VSC–HVDC cables are listed in Appendix Table II, and (14) can also be used to calculate the cable capital cost. The power loss cost of VSC–HVDC cables and its efficiency in transmission are given in (17) and (18).

$$RLC_{\text{VSCHVDC}} = 2\left(\frac{S_{\text{TT}} \cdot F \cdot \vartheta_{\text{offC}}}{nc_{\text{c}} \cdot 2\ V_{\text{cn}}}\right)^2 r_{\text{c}} \cdot l_{\text{c}} \cdot nc_{\text{c}} \cdot T_{\text{p}} \delta_{\text{op}} E = \left(\frac{S_{\text{TT}} \cdot F \cdot \vartheta_{\text{offC}}}{V_{\text{cn}}}\right)^2 \frac{r_{\text{c}} \cdot l_{\text{c}}}{2nc_{\text{c}}} \cdot T_{\text{p}} \delta_{\text{op}} E \quad (17)$$

$$\vartheta_{\text{CVSCHVDC}} = \frac{S_{\text{TT}} \cdot F \cdot \vartheta_{\text{offC}} - \left(\frac{S_{\text{TT}} \cdot F \cdot \vartheta_{\text{offC}}}{V_{\text{cn}}}\right)^2 \frac{r_{\text{c}} \cdot l_{\text{c}}}{2nc_{\text{c}}}}{S_{\text{TT}} \cdot F \cdot \vartheta_{\text{offC}}} = 1 - \frac{S_{\text{TT}} \cdot F \cdot \vartheta_{\text{offC}}}{{V_{\text{cn}}}^2} \cdot \frac{r_{\text{c}} \cdot l_{\text{c}}}{2nc_{\text{c}}} \quad (18)$$

Combining (14)–(16) and (17), (18) with the assumption values in the Nomenclature, the route costs of HVAC and VSC–HVDC systems are estimated as shown in (19) and (20) respectively.

$$\begin{aligned} RC_{\text{HVAC}} &= RCC_{\text{HVAC}} + RLC_{\text{HVAC}} \\ &= CBC_{\text{HVAC}} + CPC_{\text{HVAC}} + RLC_{\text{HVAC}} \\ &= c_{\text{c}} \cdot l_{\text{c}} \cdot nc_{\text{c}} + 0.02{V_{\text{cn}}}^2 \cdot 2\pi f_n \cdot C \cdot l_{\text{c}} + \\ &\quad 1.51767 \cdot \left(\frac{0.994 S_{\text{TT}}}{V_{\text{cn}}}\right)^2 \cdot \frac{r_{\text{c}} \cdot l_{\text{c}}}{nc_{\text{c}}} \end{aligned} \quad (19)$$

$$\begin{aligned} RC_{\text{VSCHVDC}} &= RCC_{\text{VSCHVDC}} + RLC_{\text{VSCHVDC}} \\ &= CBC_{\text{VSCHVDC}} + RLC_{\text{VSCHVDC}} \\ &= c_{\text{c}} \cdot l_{\text{c}} \cdot nc_{\text{c}} + \\ &\quad 0.75884 \cdot \left(\frac{0.983 S_{\text{TT}}}{V_{\text{cn}}}\right)^2 \cdot \frac{r_{\text{c}} \cdot l_{\text{c}}}{nc_{\text{c}}} \end{aligned} \quad (20)$$

With (9), (10) and (19), (20), the estimations of the overall costs for HVAC and VSC–HVDC systems are obtained as shown in (21) and (22).

$$\begin{aligned} C_{\text{HVAC}} &= TC_{\text{HVAC}} + RC_{\text{HVAC}} = 5 + 0.045 S_{\text{TT}} + \\ &\quad 0.02621 {S_{\text{TT}}}^{0.7513} + 0.00911 S_{\text{TT}} + \\ &\quad 0.00906 \cdot \left(S_{\text{TT}} - \frac{0.994 {S_{\text{TT}}}^2}{{V_{\text{cn}}}^2} \cdot \frac{r_{\text{c}} \cdot l_{\text{c}}}{nc_{\text{c}}}\right) + \\ &\quad c_{\text{c}} \cdot l_{\text{c}} \cdot nc_{\text{c}} + 0.02{V_{\text{cn}}}^2 \cdot 2\pi f_n \cdot C \cdot l_{\text{c}} + \\ &\quad 1.51767 \cdot \left(\frac{0.994 S_{\text{TT}}}{V_{\text{cn}}}\right)^2 \cdot \frac{r_{\text{c}} \cdot l_{\text{c}}}{nc_{\text{c}}} \end{aligned} \quad (21)$$

$$\begin{aligned} C_{\text{VSCHVDC}} &= TC_{\text{VSCHVDC}} + RC_{\text{VSCHVDC}} \\ &= 25 + 0.11 S_{\text{TT}} + 0.08148 S_{\text{TT}} + 0.02610 S_{\text{TT}} + \\ &\quad 0.02701 \cdot \left(S_{\text{TT}} - \frac{0.492 {S_{\text{TT}}}^2}{{V_{\text{cn}}}^2} \cdot \frac{r_{\text{c}} \cdot l_{\text{c}}}{nc_{\text{c}}}\right) + \\ &\quad c_{\text{c}} \cdot l_{\text{c}} \cdot nc_{\text{c}} + 0.75884 \cdot \left(\frac{0.983 S_{\text{TT}}}{V_{\text{cn}}}\right)^2 \cdot \frac{r_{\text{c}} \cdot l_{\text{c}}}{nc_{\text{c}}} \end{aligned} \quad (22)$$

B. Cost Analysis and Estimate in a LFAC System

Because there have been no commercial LFAC example to date in connection with wind energy, the capital cost of a LFAC system needs to be analyzed and estimated from the equipment in practical HVAC and VSC–HVDC projects that most closely correspond to the LFAC case.

First, on a basic view of flux and current densities, the core cross-sectional area of low frequency (LF) step-up transformers is expected to be three times larger than that of a HVAC system. However, consideration of the thermal design and insulation/bushing requirement leads instead to the view that an LF transformer could be only about $\sqrt{3}$ times of the size and weight of the standard frequency transformer in an HVAC system [30], [43], [64]. Here, the base and variable costs of the offshore platform and plant for a LFAC system are assumed to be $\sqrt{3}$ times of those for a HVAC system and the capital cost of the LFAC offshore terminal is estimated by (23).

$$TCC_{\text{offLFAC}} = \sqrt{3} B_{\text{T}} + [1 + f_{\text{T}} \cdot (n_{\text{T}} - 2)] \cdot \sqrt{3} V_{\text{T}} \cdot S_{\text{TT}} \quad (23)$$

Second, there are several possible technology options for the onshore AC-AC converter plant for a LFAC system [65], [66], such as cycloconverter [67]–[70], back-to-back modular multilevel converter [71]–[73] and modular multilevel matrix converter [74]–[77], but the choice for most cost-effective technology would be the thyristor-based cycloconverter. The circuit topology, power device number and passive component value of these AC-AC converters are a reasonably close match to the thyristor-based DC-AC converter from a CSC–HVDC (current source converter HVDC) system. The onshore plant cost in a LFAC system should be comparable to that of a CSC–HVDC onshore station and an empirical formula of which could be used for the estimation for LFAC onshore plant cost [15], [59], [78] is suggested in (24).

$$TCC_{\text{onsLFAC}} \approx TCC_{\text{onsCSCHVDC}} = 0.05926 S_{\text{TT}} \quad (24)$$

For the capitalized cost of power losses in a LFAC system, it can still use (5) and (6) to analyze and estimate the offshore power loss cost and onshore power loss cost respectively with the corresponding efficiency adjustments for offshore a LF transformer and onshore AC-AC converter.

The LF transformer volume is about $\sqrt{3}$ times the volume of a standard frequency transformer but the core losses per unit volume would be reduced at low frequency operations. Based on the theoretical analysis and simulation results in [43], [64], the efficiency of a LF transformer would be very close to a

standard transformer efficiency. For the efficiency of the onshore AC-AC converter, practical efficiency data of a thyristor-based DC-AC converter in a CSC–HVDC system [59], [79] could be used based on the same analysis for (24).

With these assumptions and relative efficiency data given in the Nomenclature, the terminal cost estimation for a LFAC system is presented in (25).

$$\begin{aligned} TC_{\text{LFAC}} &= TCC_{\text{LFAC}} + TLC_{\text{LFAC}} \\ &= TCC_{\text{offLFAC}} + TCC_{\text{onsLFAC}} + \\ &\quad TLC_{\text{offLFAC}} + TLC_{\text{onsLFAC}} \\ &= 5\sqrt{3} + 0.045\sqrt{3}S_{\text{TT}} + 0.05926S_{\text{TT}} + \\ &\quad 0.00911S_{\text{TT}} + 0.01303S_{\text{TT}} \cdot \vartheta_{\text{CLFAC}} \end{aligned} \tag{25}$$

For the compensation cost in a LFAC system, it can be seen in (11) that the reactive power produced by charging current is proportional to the operational frequency and so the required compensation power and compensation cost in a LFAC system will be theoretically one third of that in a HVAC system based on the analysis in (13).

The unit price of the subsea cable for a LFAC system is assumed to be the same as the same physical cable for a HVAC system but because of the reduced charging current and skin effect in the cable, it will have a larger transmission capability in a LFAC system than in a HVAC system. The results of a simulation and experiment [36], [80]–[82] on subsea cables identified parameters for a LFAC system are presented in Appendix Table III. The cable capital cost, power loss cost and cable efficiency calculation can follow the formulas in (14)–(16) with the corresponding parameter adjustments for a LFAC system, and its route cost estimation is given as (26).

$$\begin{aligned} RC_{\text{LFAC}} &= RCC_{\text{LFAC}} + RLC_{\text{LFAC}} \\ &= CBC_{\text{LFAC}} + CPC_{\text{LFAC}} + RLC_{\text{LFAC}} \\ &= c_{\text{c}} \cdot l_{\text{c}} \cdot nc_{\text{c}} + 0.02\ {V_{\text{cn}}}^2 \cdot 2\pi f_n \cdot C \cdot l_{\text{c}} + \\ &\quad 1.51767 \cdot \left(\frac{0.994S_{\text{TT}}}{V_{\text{cn}}}\right)^2 \cdot \frac{r_{\text{c}} \cdot l_{\text{c}}}{nc_{\text{c}}} \end{aligned} \tag{26}$$

With (25) and (26), the estimation of the overall cost for LFAC system is obtained in (27).

$$\begin{aligned} C_{\text{LFAC}} &= TC_{\text{LFAC}} + RC_{\text{LFAC}} \\ &= 5\sqrt{3} + 0.045\sqrt{3}S_{\text{TT}} + 0.00911S_{\text{TT}} + \\ &\quad 0.01303 \cdot \left(S_{\text{TT}} - \frac{0.994{S_{\text{TT}}}^2}{{V_{\text{cn}}}^2} \cdot \frac{r_{\text{c}} \cdot l_{\text{c}}}{nc_{\text{c}}}\right) + \\ &\quad c_{\text{c}} \cdot l_{\text{c}} \cdot nc_{\text{c}} + 0.02{V_{\text{cn}}}^2 \cdot 2\pi f_n \cdot C \cdot l_{\text{c}} + \\ &\quad 1.51767 \cdot \left(\frac{0.994S_{\text{TT}}}{V_{\text{cn}}}\right)^2 \cdot \frac{r_{\text{c}} \cdot l_{\text{c}}}{nc_{\text{c}}} \end{aligned} \tag{27}$$

C. Case Study for Lower Power Rating Connection

This first case study will examine a relatively low power connection case of 0.6 GW. For AC schemes (both HVAC and LFAC), it is necessary that at each distance the choice of voltage rating and cable current capacity (including use of parallel circuits) is re-examined and a minimum-cost choice made from the options available. In this study, the available cables are described in Appendix Table I for a HVAC system and Appendix Table III for a LFAC system. The analysis in (6) shows that the transmission capability of a HVAC or a LFAC cable system will fall off with the increasing distance. This is illustrated in Fig. 6 with the cable parameters in Appendix Table I and Appendix Table III. It can be seen in Fig. 6 that a LFAC system has a significant advantage over a HVAC system in terms of usable distance of a given cable based on the reduction in charging current and skin effect. For a HVDC scheme where charging current and reactive power do not apply, the cable transmission capability would not decrease with the increasing distance and so a given cable can be used over any distance for its rated transfer power.

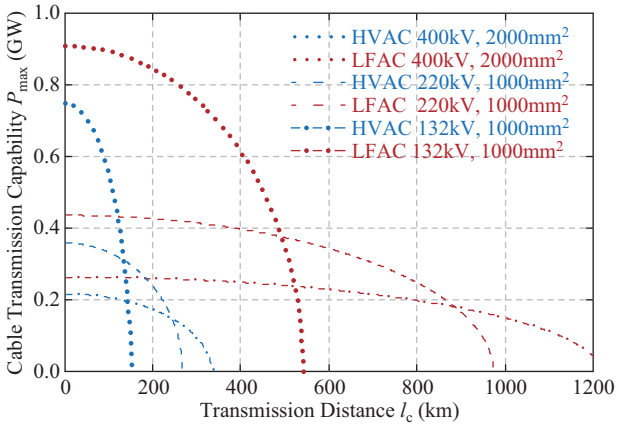

Fig. 6. Transmission capability of some common cables in HVAC and LFAC with even compensation in both ends.

Table II records the minimum-cost choices of cable made for distances up to 240 km, which is taken as the likely upper limit on offshore wind farm connections [83]–[87]. Different cable selections are made for a HVAC system to achieve the minimum cost for each distance. It is worth noting that the minimum cost selection yields the same cable for a LFAC system for all distances up to 240 km in this lower power connection case, but different cable selections will appear when power rating increases, which will be presented in the next sub-section.

The analysis in (19) and the cable choices in Table II were used to estimate the overall cost of a 0.6 GW HVAC offshore cable connection and the results are plotted in Fig. 7 for the distance ranges 0–240 km. The terminal cost is 46. 1 M£, and the route cost per unit rises rapidly with the increasing distance from 1.78 M£/km to 3.76 M£/km. The breakdown of terminal capital cost (*TCC*), route capital cost (*RCC*) terminal power loss cost (*TLC*) and route power loss cost (*RLC*) are provided in Fig. 8, and the detailed data for these constituent costs are given in Appendix Table IV. To validate the estimated costs in Fig. 7, the overall costs of two comparable connections that have been realized in practice, the 0.3 GW Capri–Torre Annunziata Interconnector in Italy and the 0.4 GW Kriegers Flak Combined Grid Interconnector between Denmark and Germany, were obtained from [88]–[91] and plotted as points P1 and P2 respectively, which, while not strictly validating the results, give reassurances that the overall cost estimation for the HVAC system are reasonable.

TABLE II
CABLE CHOICES FOR 0.6 GW CONNECTION CASE

System	Distance (km)	Voltage (kV)	Size (mm^2)	Capability per circuit (GW)	Number of circuits (n_c)
HVAC	0–65	400	1000	0.646–0.604	1
	65–80	400	1400	0.639–0.603	1
	80–120	220	800	0.320–0.300	2
	120–150	220	1000	0.321–0.299	2
	150–200	220	630	0.255–0.205	3
	200–215	220	800	0.225–0.203	3
	215–230	132	800	0.158–0.150	4
	230–240	132	1000	0.157–0.151	4
LFAC	0–240	400	800	0.733–0.685	1
VSC-HVDC	0–240	± 300	1000	0.986	1

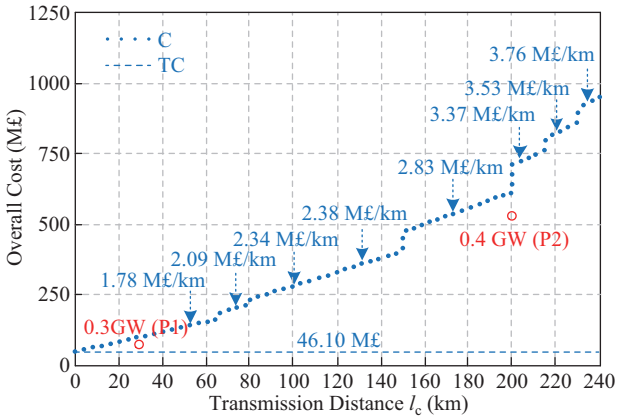

Fig. 7. Overall cost estimate of a 0.6 GW HVAC system (P1: 0.3 GW Capri–Torre Annunziata Interconnector in Italy; P2: 0.4 GW Kriegers Flak Combined Grid Interconnector between Denmark and Germany).

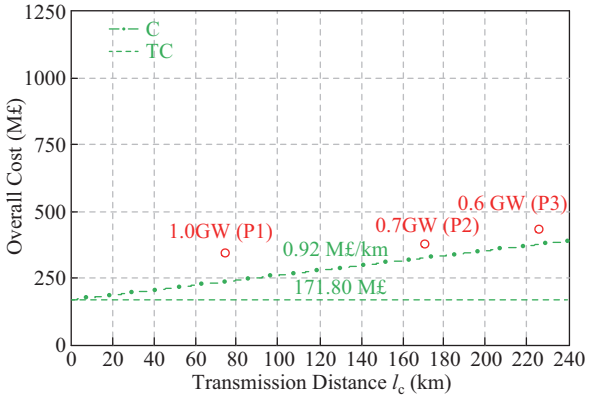

Fig. 9. Overall cost estimate of a 0.6 GW VSC–HVDC system (P1: 1 GW ElecLink Interconnector between UK and France; P2: 0.7 GW Kontek2 Interconnector between Denmark and Germany; P3: 0.6 GW ELMED Interconnector between Italy and Tunisia).

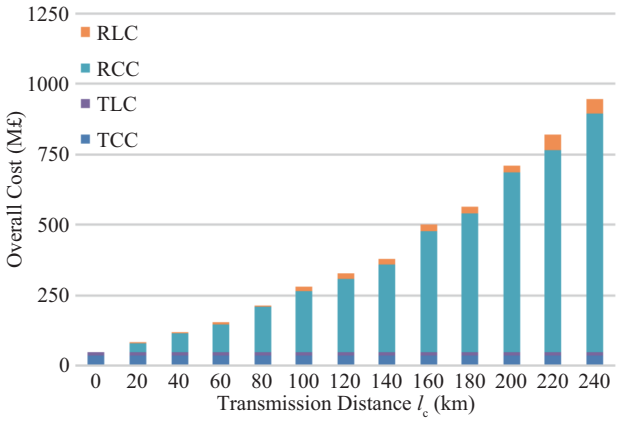

Fig. 8. Constituent costs of a 0.6 GW HVAC system.

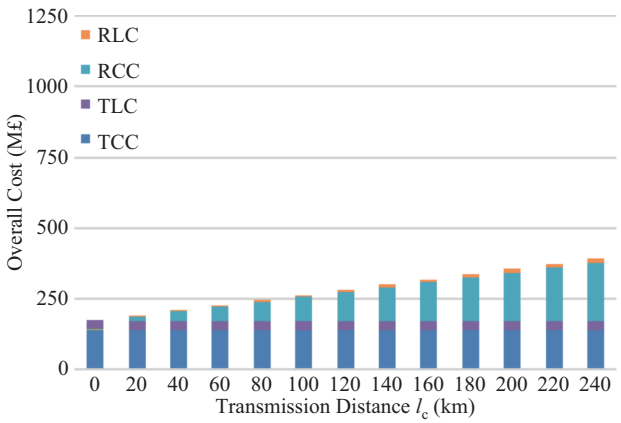

Fig. 10. Constituent costs of a 0.6 GW VSC–HVDC system.

Cost estimation for 0.6 GW VSC–HVDC offshore cable connection were produced from (20) and plotted in Fig. 9. The terminal cost is 171. 8 M£, and the route cost per unit distance maintains the same value at 0.92 M£/km for all distances up to 240 km. The detailed constituent costs are recorded in Fig. 10 and Appendix Table V. Cost data for three commercial and comparable connections, the 1.0 GW ElecLink Interconnector between UK and France, the 0.7 GW Kontek2 Interconnector between Denmark and Germany and the 0.6 GW ELMED Interconnector between Italy and Tunisia were obtained [92]–[95] and plotted as P1, P2 and P3 respectively in Fig. 9, which provides reassurance for the overall cost estimation of a VSC–HVDC system.

The cost estimation for a LFAC system based on (25) are presented in Fig. 11, Fig. 12 and Appendix Table VI. The terminal cost is 104. 2 M£, and the route cost per unit distance is maintained at 1.51 M£/km for all distances up to 240 km. There are no practically realized LFAC offshore connections to use for validation. However, the costs of individual items were estimated from similar HVAC and HVDC items and these were partially validated in the comparisons of Fig. 7 and Fig. 9.

Comparison results of these three technologies are provided in Fig. 13(a) for the distance ranges 0–240 km, and a detailed view of the ranges 65–125 km given in Fig. 13(b). It can

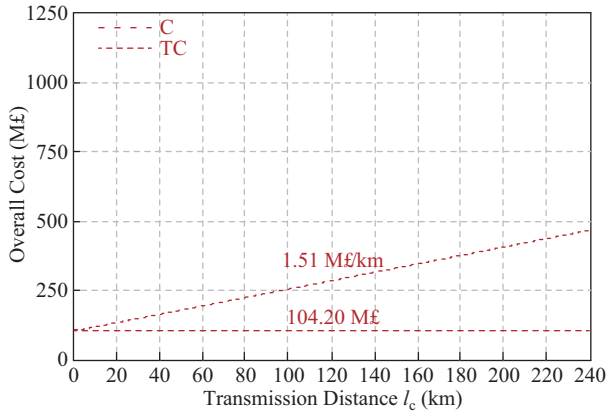

Fig. 11. Cost estimate of a 0.6 GW LFAC system.

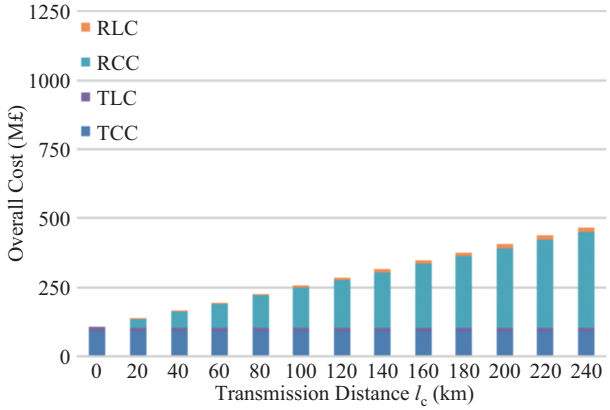

Fig. 12. Constituent costs of a 0.6 GW LFAC system.

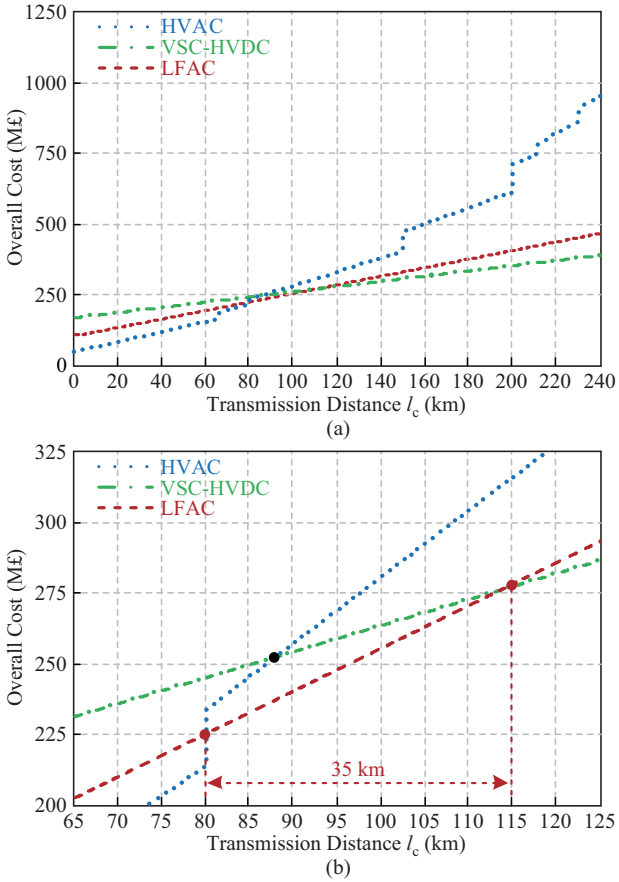

Fig. 13. 0.6 GW overall cost comparison among HVAC, VSC–HVDC and LFAC system. (a) Full distance comparison. (b) Detailed view for the cross-over and break-even points.

be seen that the overall cost of a LFAC system crosses the overall cost of a HVAC system at 80 km before crossing the overall cost of HVDC at 115 km, giving a range of 35 km over which LFAC is the least-cost solution and the percentage of overall cost advantage over both HVAC and HVDC is about 10% in this case. The terminal cost of a LFAC system is approximately halfway between that of the HVAC and HVDC systems. The route cost per unit distance of a HVAC system changes several times as the cable choice changes but beyond 65 km the route of a LFAC system lies closer to a HVDC system than to a HVAC system and this condition corresponds to the cases 1 and 2 in Fig. 4. The cross-over point of HVAC and VSC–HVDC costs is at 87 km, which is close to the value expected given the commercial project data available [19]–[21] and gives reassurance that the cost curves are realistic.

D. Case Study for Higher Power Rating Connection

A wind power connection of 1.4 GW was chosen for the higher power rating case study. The minimum-cost choices of cable for each of the three schemes are recorded in Table III.

The estimated overall cost and their constituent costs of each connection technology are plotted in Fig. 14–Fig. 19, and the

TABLE III
CABLE CHOICES FOR 1.4 GW CONNECTION CASE

System	Distance (km)	Voltage (kV)	Size (mm^2)	Capability per circuit (GW)	Number of circuits (n_c)
HVAC	0–30	400	1600	0.718–0.703	2
	30–50	400	2000	0.732–0.703	2
	50–115	400	800	0.580–0.471	3
	115–130	400	1000	0.503–0.458	3
	130–150	220	800	0.294–0.280	5
	150–170	220	800	0.297–0.279	5
	170–195	220	800	0.260–0.232	6
	195–215	220	800	0.232–0.203	7
	215–230	220	800	0.203–0.176	8
	230–240	132	800	0.150–0.145	10
LFAC	0–200	400	800	0.733–0.685	2
	200–240	400	1000	0.749–0.733	2
VSC-HVDC	0–240	± 300	2000	1.444	1

detailed cost data are given in Appendix Table VII–Appendix Table X.

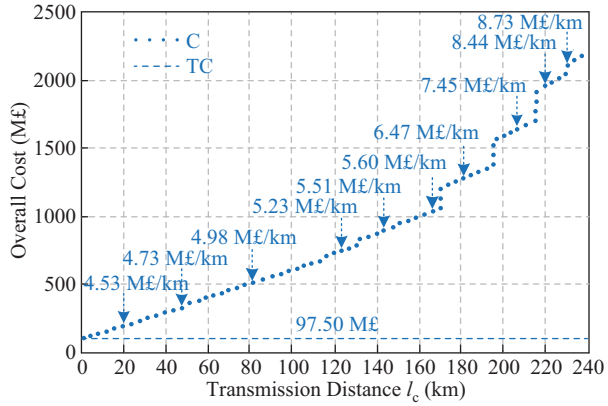

Fig. 14. Overall cost estimate of a 1.4 GW HVAC system.

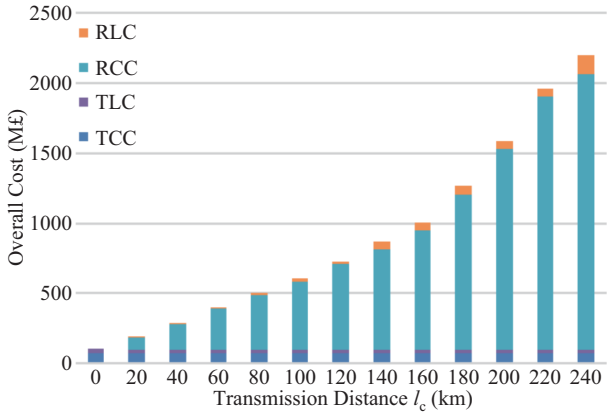

Fig. 15. Constitute costs of a 1.4 GW HVAC system.

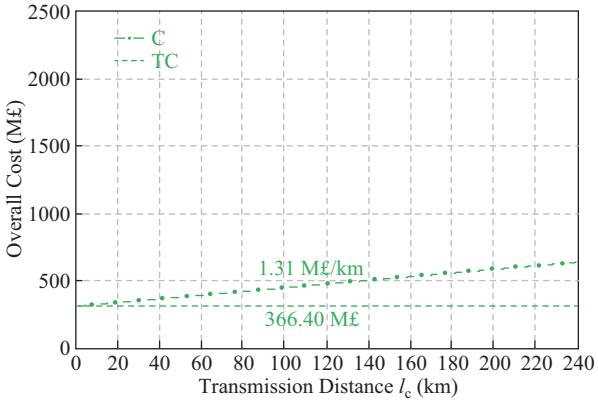

Fig. 16. Overall cost estimate of a 1.4 GW VSC–HVDC system.

The comparison result for the three technologies is provided in Fig. 20(a) over distances from 0–240 km and are shown in detail over 65–89 km in Fig. 20(b). The cross-over points of a LFAC system with HVAC and VSC–HVDC are 67 km and 79 km respectively which straddle the cross-over point of HVAC and VSC–HVDC costs at 73 km for this higher

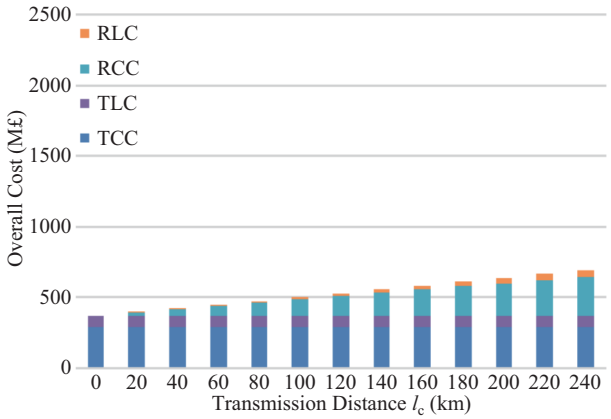

Fig. 17. Constituent costs of a 1.4 GW VSC–HVDC system.

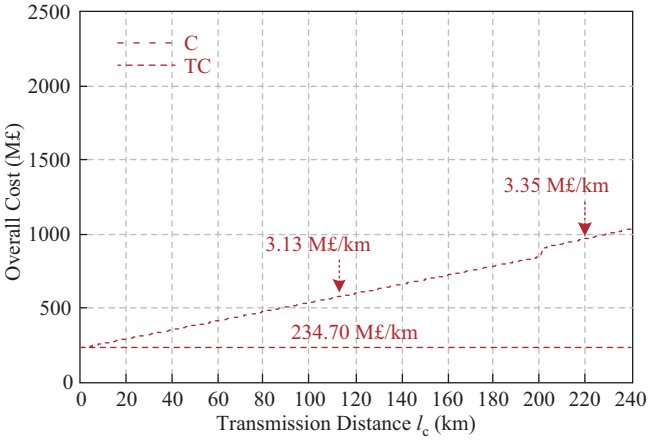

Fig. 18. Cost analysis of a 1.4 GW LFAC system.

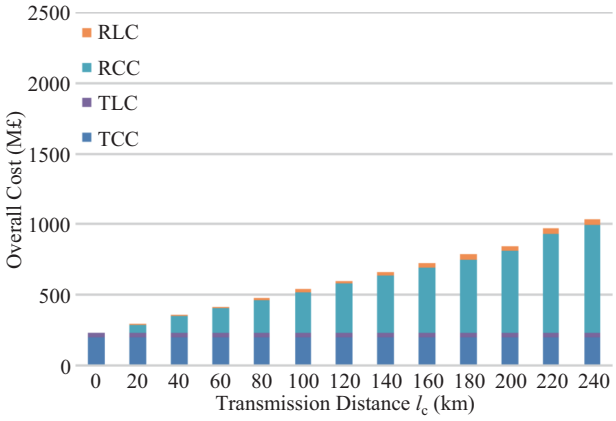

Fig. 19. Constituent costs of a 1.4 GW LFAC system.

power rating comparison. It is clear that the cost-effective range and overall cost advantage in the intermediate distance for a LFAC system is narrower at 1.4 GW than it was at 0.6 GW in Fig. 13. The terminal cost of a LFAC system is closer to that of a HVDC than HVAC system and its route cost per unit distance lies above halfway between HVDC than HVAC in the intermediate range from 50 km to 115 km. With reference to Fig. 4, at this higher power rating case study, the overall cost of LFAC starts to move from the cases 1 and 2 toward case 3.

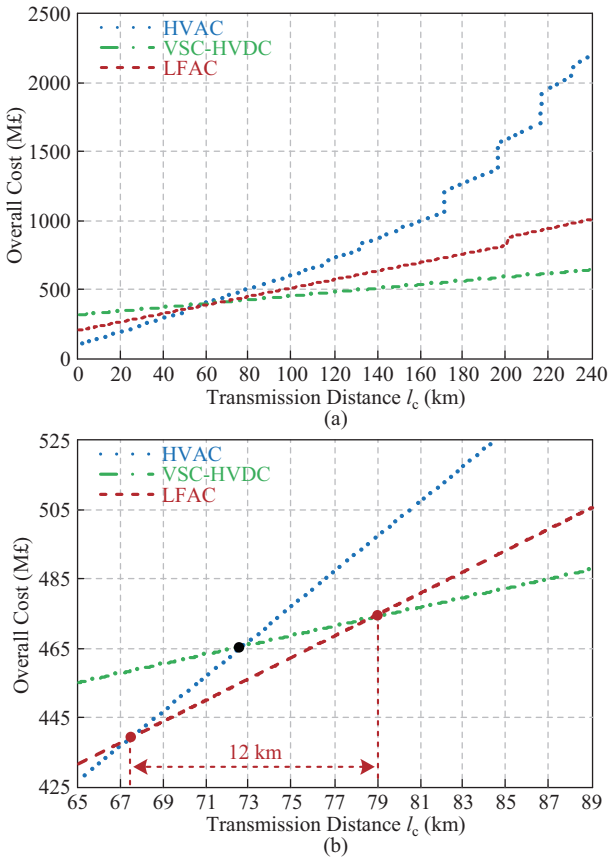

Fig. 20. 1.4 GW overall cost comparison among HVAC, VSC–HVDC and LFAC system. (a) Full distance comparison. (b) Detailed view for the cross-over and break-even points.

IV. Analysis and Estimate of A Cost-effective Range for An Onshore OHL Connection

The analysis of costs for a remote onshore OHL connection will also follow the decomposition shown in Fig. 5. *TCC* comprises the remote-end plant cost (TCC_{rem}), for instance at a wind farm site, and the load-end plant cost (TCC_{loa}). *TLC* consists of cost of power losses in the remote-end plant (TLC_{rem}) and load-end plant (TLC_{loa}). *RCC* is made up of the OHL cost (*OHC*) and compensation cost (*CPC*). *RLC* is the cost of power loss in the OHL.

A. Cost Analysis and Estimate in HVAC and CSC–HVDC Systems

The calculation and estimation for the terminal cost of HVAC and HVDC systems are based on the analysis used in the previous section. A CSC–HVDC system is selected for analysis since it is more likely to be used in the OHL connection of remote onshore wind energy than the voltage sourced alternative.

The structure of the remote-end plant and load-end plant in an OHL-based remote onshore HVAC system are similar to the onshore plant in the offshore connection case, and for which the terminal capital costs and terminal power loss costs were analyzed in (2) and (6) respectively. For a CSC–HVDC system, the estimation for its terminal capital cost and terminal power loss cost can build on (24) and (8) respectively with corresponding parameter adjustments. Thus, the calculation for the terminal cost of OHL-based HVAC and CSC–HVDC systems are provided in (28) and (29).

$$\begin{aligned} TC_{\text{HVAC}} &= TCC_{\text{HVAC}} + TLC_{\text{HVAC}} \\ &= TCC_{\text{remHVAC}} + TCC_{\text{loaHVAC}} + \\ &\quad TLC_{\text{remHVAC}} + TLC_{\text{loaHVAC}} \\ &= 2 \cdot 0.02621 {S_{\text{TT}}}^{0.7513} + 0.00911 S_{\text{TT}} + \\ &\quad 0.00906 \cdot \left(S_{\text{TT}} - \frac{0.994 {S_{\text{TT}}}^2}{{V_{\text{on}}}^2} \cdot \frac{r_{\text{o}} \cdot l_{\text{o}}}{nc_{\text{o}}} \right) \end{aligned} \tag{28}$$

$$\begin{aligned} TC_{\text{CSCHVDC}} &= TCC_{\text{CSCHVDC}} + TLC_{\text{CSCHVDC}} \\ &= TCC_{\text{remCSCHVDC}} + TCC_{\text{loaCSCHVDC}} + \\ &\quad TLC_{\text{remCSCHVDC}} + TLC_{\text{loaCSCHVDC}} \\ &= 2 \cdot 0.05926 S_{\text{TT}} + 0.01331 S_{\text{TT}} + \\ &\quad 0.01319 \cdot \left(S_{\text{TT}} - \frac{0.496 {S_{\text{TT}}}^2}{{V_{\text{on}}}^2} \cdot \frac{r_{\text{o}} \cdot l_{\text{o}}}{nc_{\text{o}}} \right) \end{aligned} \tag{29}$$

The main differences in analysis between the remote onshore OHL case and offshore cable case lies in the route cost. The analysis of transmission capability for a HVAC system is different because for the subsea cable, the effects of the shunt capacitive susceptance dominate, whereas for OHL the effects of the series inductive reactance dominate. The thermal limit described in (30) and the stability limit in (31) are the key determinants of the active power transfer capability for a given OHL-based HVAC system [39], [96]. The thermal limit applies over short distances and the stability limit for longer distances.

$$P_{\text{thl}} = 3 \frac{V_{\text{on}}}{\sqrt{3}} I_{\text{on}} = \sqrt{3} V_{\text{on}} I_{\text{on}} \tag{30}$$

$$P_{\text{stl}} = 3 \left(\frac{V_{\text{on}}}{\sqrt{3}} \right)^2 \cdot \frac{1}{X_{\text{o}}} = \frac{{V_{\text{on}}}^2}{2\pi f_n \cdot L \cdot l_{\text{o}}} \tag{31}$$

where P_{thl} and P_{stl} are the thermal limit and stability limit in OHL transmission, V_{on} and I_{on} are the OHL nominal voltage and current, X_{o} is the series reactance per kilometre, L is the OHL inductance per kilometer and l_{o} is the OHL length.

The parameters of a typical OHL in a HVAC system are listed in Appendix Table X. Their capital costs and operational power loss costs follow (14) and (15) respectively and the calculation for the route cost of an OHL-based HVAC system is given in (32).

$$\begin{aligned} RC_{\text{HVAC}} &= RCC_{\text{HVAC}} + RLC_{\text{HVAC}} = c_{\text{o}} \cdot l_{\text{o}} \cdot nc_{\text{o}} + \\ &\quad 1.51767 \cdot \left(\frac{0.994 S_{\text{TT}}}{V_{\text{on}}} \right)^2 \cdot \frac{r_{\text{o}} \cdot l_{\text{o}}}{nc_{\text{o}}} \end{aligned} \tag{32}$$

where c_{o} is the OHL cost per set including supply and installation, nc_{o} is the number of OHL parallel circuits and r_{o} is the OHL resistance per kilometer.

The stability limit imposed by the inductive reactance in HVAC has no relevance to the HVDC case. A thermal limit does still apply but here HVDC has an advantage because the line can be used consistently at its peak voltage and does not suffer an effective/peak ratio underutilization. The parameters of the typical CSC–HVDC OHL are listed in

Appendix Table XI, and the route cost for an OHL-based CSC–HVDC system is given by (33) based on (14) and (17).

$$RC_{\text{CSCHVDC}} = RCC_{\text{CSCHVDC}} + RLC_{\text{CSCHVDC}} = c_{\text{o}} \cdot l_{\text{o}} \cdot nc_{\text{o}} + 0.75884 \cdot \left(\frac{0.991 S_{\text{TT}}}{V_{\text{on}}}\right)^2 \cdot \frac{r_{\text{o}} \cdot l_{\text{o}}}{nc_{\text{o}}} \quad (33)$$

Summing the terminal costs and route costs yields the estimates of overall costs. Adding (28) and (32) gives (34) for a HVAC system and adding (29) and (33) gives (35) for a CSC–HVDC system.

$$\begin{aligned} C_{\text{HVAC}} &= TC_{\text{HVAC}} + RC_{\text{HVAC}} \\ &= 2 \cdot 0.02621 {S_{\text{TT}}}^{0.7513} + 0.00911 S_{\text{TT}} + \\ &\quad 0.00906 \cdot \left(S_{\text{TT}} - \frac{0.994 {S_{\text{TT}}}^2}{{V_{\text{on}}}^2} \cdot \frac{r_{\text{o}} \cdot l_{\text{o}}}{nc_{\text{o}}}\right) + \\ &\quad c_{\text{o}} \cdot l_{\text{o}} \cdot nc_{\text{o}} + 1.51767 \cdot \left(\frac{0.994 S_{\text{TT}}}{V_{\text{on}}}\right)^2 \cdot \frac{r_{\text{o}} \cdot l_{\text{o}}}{nc_{\text{o}}} \end{aligned} \quad (34)$$

$$\begin{aligned} C_{\text{CSCHVDC}} &= TC_{\text{CSCHVDC}} + RC_{\text{CSCHVDC}} \\ &= 2 \cdot 0.05926 S_{\text{TT}} + 0.01331 S_{\text{TT}} + \\ &\quad 0.01319 \cdot \left(S_{\text{TT}} - \frac{0.496 {S_{\text{TT}}}^2}{{V_{\text{on}}}^2} \cdot \frac{r_{\text{o}} \cdot l_{\text{o}}}{nc_{\text{o}}}\right) + \\ &\quad c_{\text{o}} \cdot l_{\text{o}} \cdot nc_{\text{o}} + 0.75884 \cdot \left(\frac{0.991 S_{\text{TT}}}{V_{\text{on}}}\right)^2 \cdot \frac{r_{\text{o}} \cdot l_{\text{o}}}{nc_{\text{o}}} \end{aligned} \quad (35)$$

B. Cost Analysis and Estimate in a LFAC System

Building on the analysis in (28) and (29) for HVAC and CSC–HVDC systems, the terminal cost for a LFAC system can be estimated by (36).

$$\begin{aligned} TC_{\text{LFAC}} &= TCC_{\text{LFAC}} + TLC_{\text{LFAC}} \\ &= TCC_{\text{remLFAC}} + TCC_{\text{loaLFAC}} + \\ &\quad TLC_{\text{remLFAC}} + TLC_{\text{loaLFAC}} \\ &= 0.02621\sqrt{3} {S_{\text{TT}}}^{0.7513} + \\ &\quad 0.05926 S_{\text{TT}} + 0.00911 S_{\text{TT}} + \\ &\quad 0.01323 \cdot \left(S_{\text{TT}} - \frac{0.994 {S_{\text{TT}}}^2}{{V_{\text{on}}}^2} \frac{r_{\text{o}} \cdot l_{\text{o}}}{nc_{\text{o}}}\right) \end{aligned} \quad (36)$$

For the route cost of LFAC, the price per unit distance of the OHL is assumed to be the same as for HVAC but, as (31) suggests, the stability limit in LFAC is expected to be at a distance three times that of HVAC assuming a frequency reduction to one third. The parameters of onshore OHL LFAC can be taken from the simulation and experimental results [39], [42], [97], and are presented in Appendix Table XII, and the route cost for an OHL-based LFAC system is provided in (37).

$$RC_{\text{LFAC}} = RCC_{\text{LFAC}} + RLC_{\text{LFAC}} = c_{\text{o}} \cdot l_{\text{o}} \cdot nc_{\text{o}} + 1.51767 \cdot \left(\frac{0.994 S_{\text{TT}}}{V_{\text{on}}}\right)^2 \cdot \frac{r_{\text{o}} \cdot l_{\text{o}}}{nc_{\text{o}}} \quad (37)$$

Adding the terminal cost and route cost of (36) and (37), yields the overall cost for a LFAC system as given in (38).

$$\begin{aligned} C_{\text{LFAC}} &= TC_{\text{LFAC}} + RC_{\text{LFAC}} \\ &= 0.02621\sqrt{3} {S_{\text{TT}}}^{0.7513} + 0.05926 S_{\text{TT}} + 0.00911 S_{\text{TT}} + \\ &\quad 0.01323 \cdot \left(S_{\text{TT}} - \frac{0.994 {S_{\text{TT}}}^2}{{V_{\text{on}}}^2} \frac{r_{\text{o}} \cdot l_{\text{o}}}{nc_{\text{o}}}\right) + c_{\text{o}} \cdot l_{\text{o}} \cdot nc_{\text{o}} + \\ &\quad 1.51767 \cdot \left(\frac{0.994 S_{\text{TT}}}{V_{\text{on}}}\right)^2 \cdot \frac{r_{\text{o}} \cdot l_{\text{o}}}{nc_{\text{o}}} \end{aligned} \quad (38)$$

C. Case Study for Lower Power Rating Connection

A wind power connection of 3.0 GW was selected as an example of a relatively lower power rating case study. Following Sections III-C and III-D, the choice of voltage rating and OHL current capacity should be re-examined at each distance for AC schemes and a minimum-cost choice can be made from the options available. In this study, the available OHL are given in Appendix Table X for a HVAC system and Appendix Table XII for a LFAC system. According to the analysis in (30) and (31), it is the thermal limit that is relevant for HVAC and LFAC systems applied over short distances, and beyond this, the stability limit is the constraInternational The change-over distance between the limitations is greater for LFAC than HVAC, and this is clear from the results in Fig. 21 and with the parameters in Appendix Table X and Appendix Table XII. It can be seen that a LFAC system has a clear advantage over a HVAC system due to the reduced impact of skin effect for the thermal limit and the one-third series reactance which extends the stability limit. It also illustrates that since the thermal limit is irrelevant to the transmission distance while the reliability limit is relevant, the constant transmission capacity over shorter distances and the declining capacity over longer distances can be observed for OHL-based AC schemes. For a DC scheme, a CSC–HVDC system does not suffer from effects of the series inductive reactance and the transmission capability is set by the thermal limit at all distances.

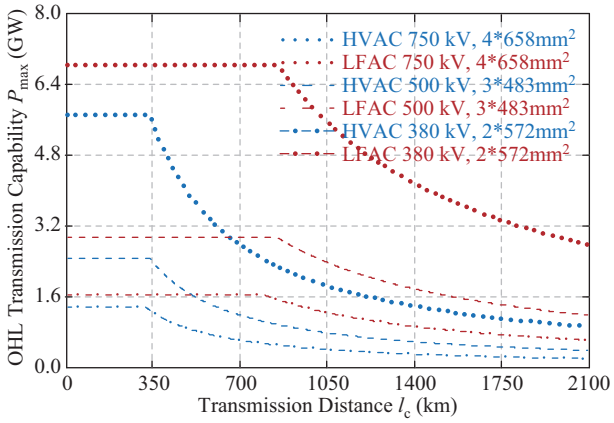

Fig. 21. Transmission capability of some typical OHL in HVAC and L.

Table IV records the minimum-cost choices of OHL made for distances up to 1500 km, which is representative of remote onshore wind farm locations [83]–[87].

Using the OHL choices in Table IV, and the analysis of (32), (33) and (36), the estimated overall cost of a 3.0 GW remote onshore OHL connection via HVAC, CSC–HVDC and LFAC was calculated over 0–1500 km. The results are plotted

TABLE IV
OHL CHOICES FOR 3.0 GW CONNECTION CASE

System	Distance (km)	Voltage (kV)	Capability per circuit (GW)	Number of circuits (n_c)
HVAC	0–645	750	5.690–3.007	1
	645–1290	750	3.007–1.504	2
	1290–1500	750	1.504–1.293	3
LFAC	0–1500	750	6.819–3.879	2
CSC-HVDC	0–1500	± 600	6.564	1

in Fig. 22–Fig. 27 and further details are provided in Appendix Table XIII–Appendix Table XV.

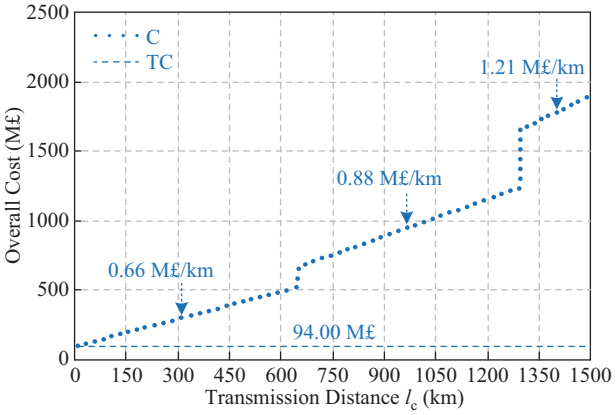

Fig. 22. Overall cost estimate of a 3.0 GW HVAC system.

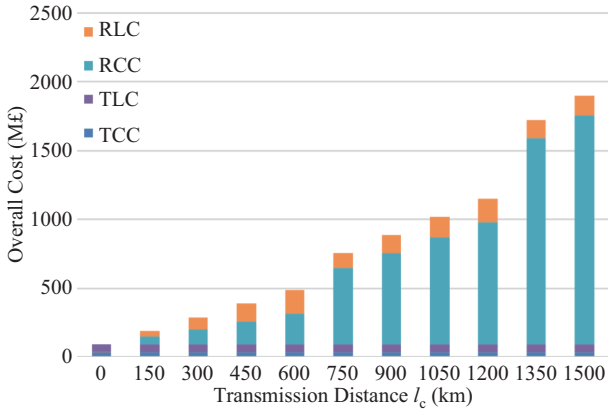

Fig. 23. Constituent costs of a 3.0 GW HVAC system.

The comparison result is given in Fig. 28(a) for the distance from 0–1500 km, and a detailed view of 600-1000 km is provided in Fig. 28(b). The cross-over points of a LFAC system with HVAC and CSC–HVDC are 650 km and 960 km respectively, giving a cost-effective range of 310 km in the intermediate distance and the overall cost advantage over both HVAC and HVDC is close to 15% in this case study. It can be seen that the terminal cost of a LFAC system is approximately midway between that of the HVAC and HVDC systems. The route cost is a relatively complex picture because the unit cost of AC increases with distance as the stability limit grows in significance and this happens more so in standard frequency than low frequency. For distances below 650 km, the route cost per unit distance of LFAC and HVAC are

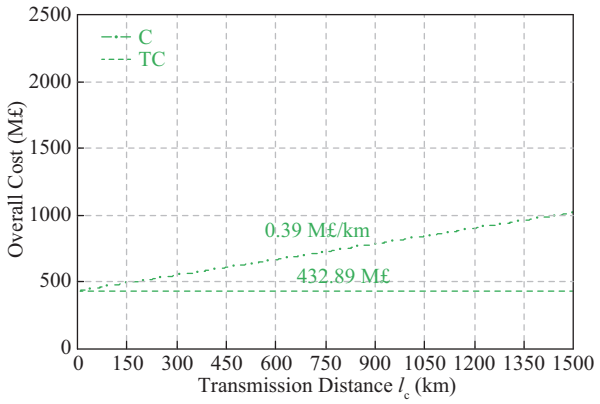

Fig. 24. Overall cost estimate of a 3.0 GW CSC–HVDC system.

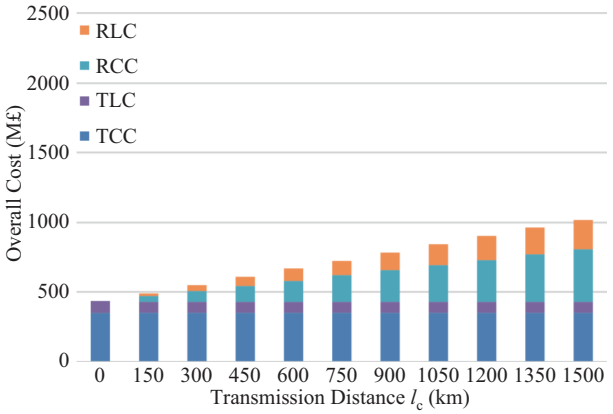

Fig. 25. Constituent costs of a 3.0 GW HVDC system.

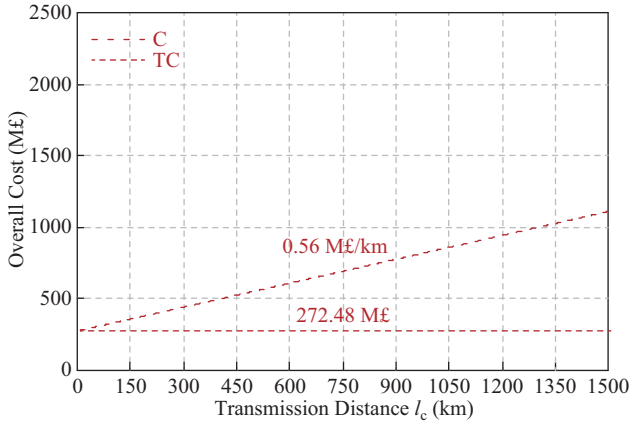

Fig. 26. Overall cost estimate of a 3.0 GW LFAC system.

similar but beyond that the route cost of HVAC rises rapidly as parallel circuits are required whereas a single circuit suffices for LFAC all the way to 1500 km and so the route cost of LFAC lies closer to HVDC than to HVAC after 650 km. The overall cost of a LFAC system in this OHL-based lower power connection belongs to a situation between case 1 and case 2 as shown in Fig. 4. The break-even point of HVAC and CSC–HVDC is 700 km, which reaches good agreement with the practical result in the commercial OHL-based remote onshore connection projects [22], [23].

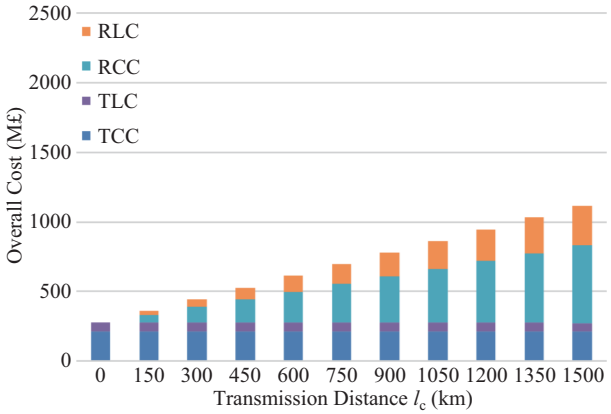

Fig. 27. Constituent costs of a 3.0 GW LFAC system.

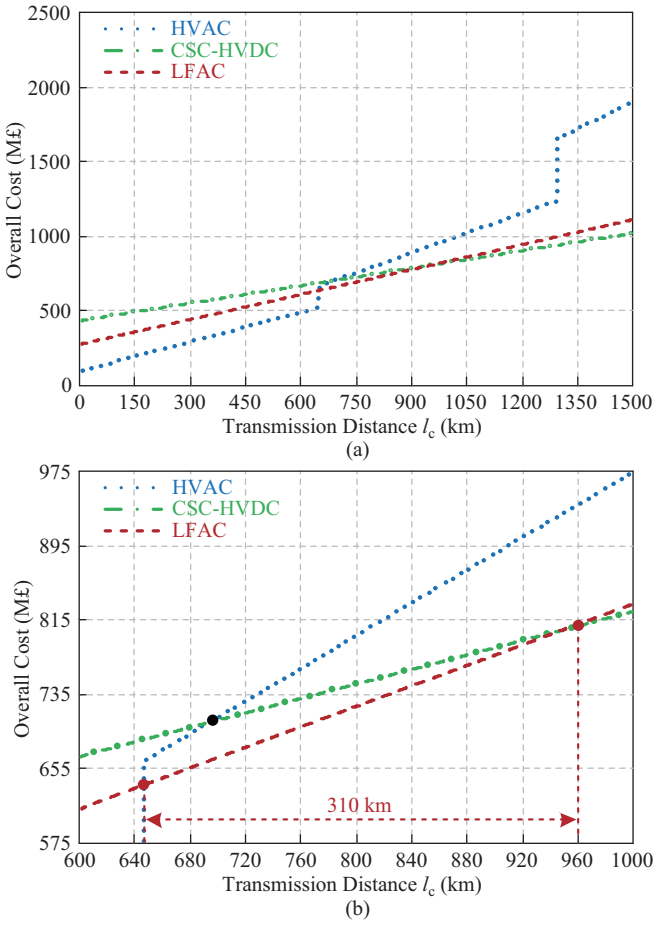

Fig. 28. 3.0 GW overall cost comparison among HVAC, CSC–HVDC and LFAC systems. (a) Full distance comparison. (b) Detailed view for the cross-over and break-even points.

D. Case Study for Higher Power Rating Connection

A power connection of 5.0 GW was chosen for the higher power rating case study. The minimum-cost choices of OHL for each of the three technologies over 0–1500 km are presented in Table V.

The estimated overall costs of each technology choice at 5.0 GW connection are plotted in Fig. 29–Fig. 34 and the details of the constituent costs are given in Appendix Table XVI–Appendix Table XVIII.

TABLE V
OHL CHOICES FOR 5.0 GW CONNECTION CASE

System	Distance (km)	Voltage (kV)	Capability per circuit (GW)	Number of circuits (n_c)
HVAC	0–775	750	5.690–2.503	2
	775–1164	750	2.503–1.666	3
	1164–1500	750	1.666–1.293	4
LFAC	0–1164	750	6.819–4.999	1
	1164–1500	750	4.999–3.879	2
CSC-HVDC	0–1500	± 600	6.564	1

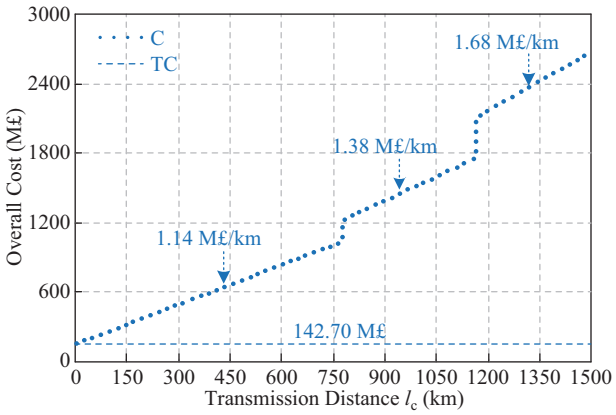

Fig. 29. Overall cost estimate of a 5.0 GW HVAC system.

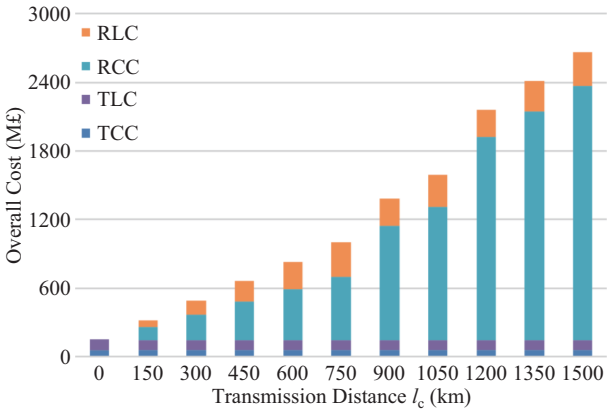

Fig. 30. Constituent costs of a 5.0 GW HVAC system.

The comparison results are provided in Fig. 35(a) over the whole distance with details over 750–1000 km in Fig. 35(b). It shows the cross-over points of the LFAC overall cost with HVAC and CSC–HVDC are 775 km and 965 km respectively which straddle the cross-over point of HVAC and CSC–HVDC overall costs at 790 km. The cost-effective range for LFAC is narrowed to 190 km at this 5.0 GW comparison whereas it was 310 km at 3.0 GW comparison, and the percentage of overall cost advances is also reduced in this case study. In this higher power connection case, the terminal cost of a LFAC system is between that of HVAC and HVDC but becomes closer to HVDC. The unit route cost per unit distance of LFAC is higher than the midpoint of the HVAC and CSC–HVDC systems in the intermediate range and shows one increase at

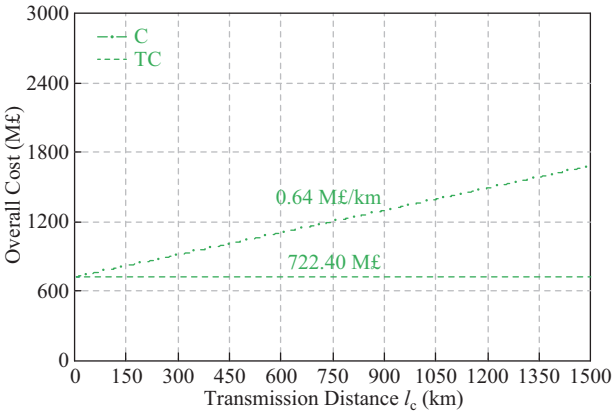

Fig. 31. Overall cost estimate of a 5.0 GW CSC–HVDC system.

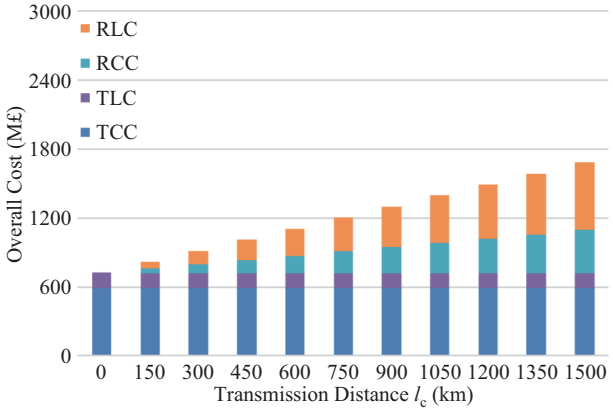

Fig. 32. Constituent costs of a 5.0 GW CSC–HVDC system.

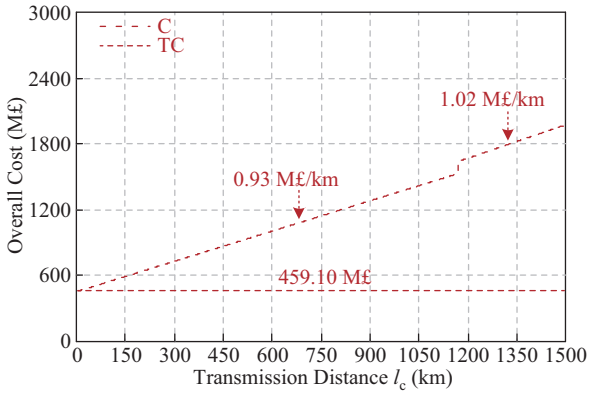

Fig. 33. Overall cost estimate of a 5.0 GW LFAC system.

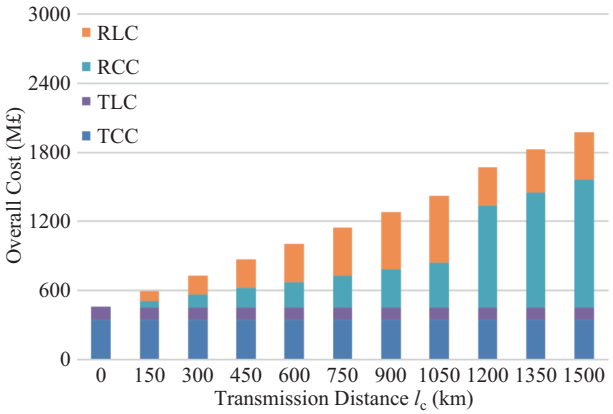

Fig. 34. Constituent costs of a 5.0 GW LFAC system.

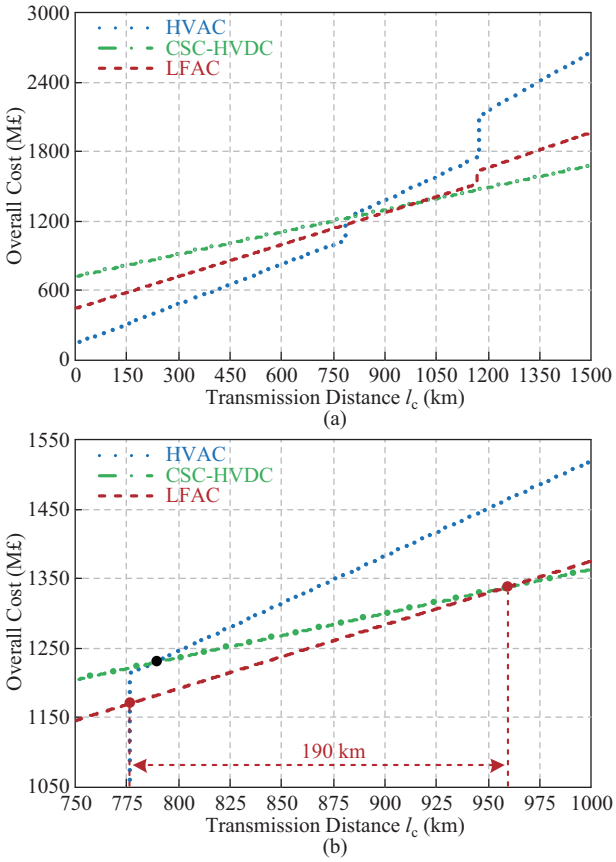

Fig. 35. 5.0 GW overall cost comparison among HVAC, CSC–HVDC and LFAC systems. (a) Full distance comparison of. (b) Detailed view for the cross-over and break-even points.

1164 km because of a need to move to two parallel circuits. This comparison results belong to a situation between the case 2 and case 3 of Fig. 4.

V. Discussion of Cost-effective Distance

The cross-over points of overall costs between HVAC, HVDC and LFAC in the four case studies of wind energy connections (lower power rating and higher power rating, offshore cable connection and remote onshore OHL connection) are summarized in Table VI. The range of cost-effective distance for the LFAC system is also recorded.

First, it can be seen that there is indeed a cost-effective range for the LFAC system over both HVAC and HVDC technologies in the intermediate distance for all the four cases of wind energy connection.

Second, it can be determined that the cost-effective range narrows with increasing power rating for both offshore cable connections and remote onshore OHL connections. The narrowing of the cost-effective range with an increasing power rating can be explained by reference to the detailed constituent

TABLE VI
SUMMARY OF CROSS-OVER POINTS AND LFAC COST-EFFECTIVE RANGES

Case study	Cross-over points of overall costs			LFAC cost-effective ranges
	LFAC-HVAC	HVDC-HVAC	HVDC-LFAC	
Cable 0.6 GW	80 km	87 km	115 km	35 km (14.5% of full length)
Cable 1.4 GW	67 km	73 km	79 km	12 km (5.0% of full length)
OHL 3.0 GW	650 km	700 km	960 km	310 km (20.7% of full length)
OHL 5.0 GW	775 km	790 km	965 km	190 km (12.7% of full length)

cost in Appendix Table VII to Appendix Table IX and Appendix Table XVI to Appendix Table XVIII. This reveals that the LFAC terminal cost approaches that of HVDC rather than HVAC at higher power case because of the expense of the AC-AC converter and LF transformer. Also, at higher power rating, the advantages of DC operations, rather than AC (standard frequency and low frequency) of both cable and OHL are greater in terms of both transmission capability and route cost.

Third, it can also be observed that the overall costs of the LFAC system are more competitive in the remote onshore OHL cases than the offshore cable cases and this is for both lower and higher power rating connections. The cost-effective ranges are larger for OHL cases than for cable cases both in absolute terms and relative to the longest distances that might be built. These differences can be explained by the different mechanisms that limit transmission capability of LFAC in cables and OHL. This will be analyzed further in the next section.

VI. TRANSMISSION CAPABILITY OF THE LFAC SYSTEM

For offshore cable case, the transmission capability is dependent on the analysis of (12). The ratio of active power transfer capability of the LFAC system to HVAC system can be expressed as (39). Taking skin effect into consideration, the rated current of a given cable under the LFAC system would be about 1.2 greater than under the HVAC system [43], [80]. In this manner, (39) can be simplified as (40) and this difference can be observed by the starting points in Fig. 6.

$$\frac{P_{\text{c-LFAC}}}{P_{\text{c-HVAC}}} = \sqrt{\frac{\left(\sqrt{3}V_{\text{cn}}I_{\text{cn-LFAC}}\right)^2 - \frac{1}{4}\left[{V_{\text{cn}}}^2 \cdot 2\pi f_{n\text{-LFAC}} \cdot C \cdot l_{\text{c}}\right]^2}{\left(\sqrt{3}V_{\text{cn}}I_{\text{cn-HVAC}}\right)^2 - \frac{1}{4}\left[{V_{\text{cn}}}^2 \cdot 2\pi f_{n\text{-HVAC}} \cdot C \cdot l_{\text{c}}\right]^2}} \tag{39}$$

$$\frac{P_{\text{c-LFAC}}}{P_{\text{c-HVAC}}} = \sqrt{\frac{4.32{I_{\text{cn-HVAC}}}^2 - \frac{1}{36}\left(V_{\text{cn}} \cdot 2\pi f_{n\text{-HVAC}} \cdot C \cdot l_{\text{c}}\right)^2}{3{I_{\text{cn-HVAC}}}^2 - \frac{1}{4}\left(V_{\text{cn}} \cdot 2\pi f_{n\text{-HVAC}} \cdot C \cdot l_{\text{c}}\right)^2}} \tag{40}$$

From (40), this ratio has a minimum value of 1.2 if no compensation current is needed and the ratio will increase with the compensation current. In short distance transmission, the compensation current would not normally exceed the active power current [21], [57], [63] which yields a maximum ratio of 1.7 as given by (41), so the ratio of active power transfer capability of the LFAC system to HVAC system would be between 1.2 and 1.7.

$$\begin{aligned}\frac{P_{\text{c-LFAC}}}{P_{\text{c-HVAC}}} &= \sqrt{\frac{4.32{I_{\text{cn-HVAC}}}^2 - \frac{1}{36}\left(\sqrt{3}I_{\text{ch}}\right)^2}{3{I_{\text{cn-HVAC}}}^2 - \frac{1}{4}\left(\sqrt{3}I_{\text{ch}}\right)^2}} \\ &= \sqrt{\frac{4.32{I_{\text{cn-HVAC}}}^2 - \frac{1}{36}\left(2\sqrt{3}I_{\text{Qoff}}\right)^2}{3{I_{\text{cn-HVAC}}}^2 - \frac{1}{4}\left(2\sqrt{3}I_{\text{Qoff}}\right)^2}} \\ &= \sqrt{\frac{4.32{I_{\text{cn-HVAC}}}^2 - \frac{1}{3}{I_{\text{Qoff}}}^2}{3{I_{\text{cn-HVAC}}}^2 - 3{I_{\text{Qoff}}}^2}} \\ &\leqslant \sqrt{\frac{4.32{I_{\text{cn-HVAC}}}^2 - \frac{1}{6}{I_{\text{cn-HVAC}}}^2}{3{I_{\text{cn-HVAC}}}^2 - \frac{3}{2}{I_{\text{cn-HVAC}}}^2}} \approx 1.7\end{aligned} \tag{41}$$

where I_{ch} is the capacitive charging current in the subsea cable and I_{Qoff} is the offshore compensation current.

For the remote onshore OHL case, the same assumption for skin effect is made for direct comparison with the cable case. In short distances, the OHL transmission capability is thermally limited and the ratio between the LFAC to HVAC system is 1.2 as the starting points shown in Fig. 21. When the distance increases beyond some critical point, the OHL transmission capability is governed by the stability limit which is the curved section of Fig. 21 based on the analysis in (31), and the ratio between the LFAC to HVAC system becomes 3 as shown in (42).

$$\frac{P_{\text{o-LFAC}}}{P_{\text{o-HVAC}}} \leqslant \frac{\frac{{V_{\text{on}}}^2}{2\pi f_{n\text{-LFAC}} \cdot L \cdot l_{\text{o}}}}{\frac{{V_{\text{on}}}^2}{2\pi f_{n\text{-HVAC}} \cdot L \cdot l_{\text{o}}}} = \frac{f_{n\text{-HVAC}}}{f_{n\text{-LFAC}}} = 3 \tag{42}$$

Comparing the offshore cable and remote onshore OHL cases, the LFAC system could give a greater transmission capability enhancement in OHL than that in cables, and as a result, the benefit-cost ratio will be better for the OHL system than cable system, which may imply that LFAC would find more potential in remote onshore OHL applications than offshore cable applications.

VII. CONCLUSION

This paper presented an in-depth analysis for the overall cost of a LFAC system and then gave an extensive comparison with HVAC and HVDC to explore the distances range of over which LFAC is more cost-effective over both HVAC and HVDC in connections of offshore and remote onshore wind energy.

First, the overall cost of a LFAC system was decomposed into constituent costs of terminal and route costs and further decomposed into capital and operational costs. Then, equations for evaluating these constituent costs were elaborated. Given the absence of commercial LFAC projects that might yield cost data, parameters for the cost equations for the LFAC system were estimated with reference to similar equipment used in HVDC and HVAC practices. Lastly, the cost estimation algorithm compared different choices of operating voltage, conductor size and number of circuits in order to identify the lowest cost combination at each distance for the specified

power transfer and provide a fair comparison for these three technology choices.

Graphs of costs against distance for offshore cable and remote onshore OHL cases and for lower and higher power connection cases have been created. The results have demonstrated that the LFAC system does possess distance ranges over which it is expected to be more cost-effective than both HVAC and HVDC systems. The overall cost advantage of LFAC is generally larger in the OHL connection of remote onshore wind energy than the cable connection of offshore wind energy, and it is more competitive for a lower power rating connection than higher power rating connection in both the cable and OHL cases.

APPENDIX

Appendix TABLE I
PARAMETERS OF THE COMMON CABLES IN A HVAC SYSTEM

Nominal Voltage V_n (kV)	Cable size (mm^2)	Resistance r_c (mΩ/km)	Capacitance C (nF/km)	Nominal Current I_n (A)	Cables cost c_c (k£/km)
132	500	49.3	192	739	635
	630	39.5	209	818	685
	800	32.4	217	888	795
	1000	27.5	238	949	860
220	500	48.9	136	732	815
	630	39.1	151	808	850
	800	31.9	163	879	975
	1000	27.0	177	942	1000
400	800	31.4	130	870	1400
	1000	26.5	140	932	1550
	1200	22.1	170	986	1700
	1400	18.9	180	1015	1850
	1600	16.6	190	1036	2000
	2000	13.2	200	1078	2150

Appendix TABLE II
PARAMETERS OF THE COMMON CABLES IN A VSC–HVDC SYSTEM

Nominal Voltage V_n (kV)	Cable size (mm^2)	Resistance r_c (mΩ/km)	Nominal Current I_n (A)	Cables cost c_c (k£/km)
± 150	1000	22.4	1644	670
	1200	19.2	1791	730
	1400	16.5	1962	785
	1600	14.4	2123	840
	2000	11.5	2407	900
± 220	1000	22.4	1644	855
	1200	19.2	1791	940
	1400	16.5	1962	1015
	1600	14.4	2123	1090
	2000	11.5	2407	1175

Appendix TABLE III
PARAMETERS OF THE COMMON CABLES IN A LFAC SYSTEM

Nominal Voltage V_n (kV)	Cable size (mm^2)	Resistance r_c (mΩ/km)	Capacitance C (nF/km)	Nominal Current I_n (A)	Cables cost c_c (k£/km)
132	500	32.6	192	899	635
	630	26.2	209	995	685
	800	21.5	217	1080	795
	1000	18.2	238	1154	860
220	500	32.4	136	890	815
	630	25.9	151	982	850
	800	21.1	163	1069	975
	1000	17.9	177	1145	1000
400	800	20.8	130	1058	1400
	1000	17.5	140	1133	1550
	1200	14.6	170	1199	1700
	1400	12.5	180	1234	1850
	1600	11.0	190	1260	2000
	2000	8.7	200	1310	2150

Appendix TABLE IV
DETAILED CONSTITUENT COST DATA FOR A 0.6 GW HVAC SYSTEM

HVAC		Transmission Distance l (km)												
		0	20	40	60	80	100	120	140	160	180	200	220	240
Cost (M£)	*TCC*	35.2	35.2	35.2	35.2	35.2	35.2	35.2	35.2	35.2	35.2	35.2	35.2	35.2
	TLC	10.9	10.9	10.9	10.9	10.9	10.8	10.8	10.8	10.8	10.7	10.7	10.6	10.6
	RCC	0	33.8	67.6	101.4	162.5	216.7	260.0	312.1	430.0	493.8	640.0	720.5	850.6
	RLC	0	1.8	3.6	5.4	5.1	17.8	21.4	21.1	23.3	26.2	23.8	55.3	51.2
	C	46.1	81.7	117.3	152.9	213.7	280.5	327.4	379.3	499.3	565.9	709.7	821.6	947.6

Appendix TABLE V
DETAILED CONSTITUENT COST DATA FOR A 0.6 GW VSC–HVDC SYSTEM

HVDC		Transmission Distance l (km)												
		0	20	40	60	80	100	120	140	160	180	200	220	240
Cost (M£)	*TCC*	139.6	139.6	139.6	139.6	139.6	139.6	139.6	139.6	139.6	139.6	139.6	139.6	139.6
	TLC	31.9	31.9	31.9	31.8	31.8	31.8	31.8	31.8	31.8	31.8	31.8	31.7	31.7
	RCC	0	17.1	34.2	51.3	68.4	85.5	102.6	119.7	136.8	153.9	171	188.1	205.2
	RLC	0	1.3	2.6	3.9	5.3	6.6	7.9	9.2	10.5	11.8	13.2	14.5	15.7
	C	171.5	189.9	208.3	226.6	245.1	263.5	281.9	300.3	318.7	337.1	355.6	373.9	392.2

Appendix TABLE VI
DETAILED CONSTITUENT COST DATA FOR A 0.6 GW LFAC SYSTEM

LFAAC		Transmission Distance l (km)												
		0	20	40	60	80	100	120	140	160	180	200	220	240
Cost (M£)	*TCC*	90.8	90.8	90.8	90.8	90.8	90.8	90.8	90.8	90.8	90.8	90.8	90.8	90.8
	TLC	13.4	13.3	13.4	13.4	13.4	13.3	13.3	13.3	13.3	13.3	13.3	13.3	13.3
	RCC	0	28.9	57.7	86.6	115.5	144.4	173.2	202.1	231.0	259.8	288.7	317.6	346.5
	RLC	0	1.4	2.8	4.2	5.6	7.0	8.4	9.8	11.2	12.7	14.1	15.5	16.9
	C	104.2	134.4	164.7	195.0	225.3	255.5	285.7	316.0	346.3	376.6	406.9	437.2	467.5

Appendix TABLE VII
DETAILED CONSTITUENT COST DATA FOR A 1.4 GW HVAC SYSTEM

HVAC		Transmission Distance l (km)												
		0	20	40	60	80	100	120	140	160	180	200	220	240
Cost (M£)	*TCC*	73.9	73.9	73.9	73.9	73.9	73.9	73.9	73.9	73.9	73.9	73.9	73.9	73.9
	TLC	24.4	24.4	24.4	24.4	24.3	24.3	24.3	24.1	24.1	24.1	24.1	24.1	23.6
	RCC	0	87.6	184.1	290.5	387.3	484.1	608.7	717.2	853.0	1106.5	1434.4	1803.2	1965.0
	RLC	0	3.1	4.9	11.6	15.4	19.3	19.5	54.3	52.5	58.2	55.4	53.4	131.4
	C	99.5	190.2	288.5	401.6	502.1	602.8	727.6	870.7	1004.7	1263.9	1589.0	1955.8	2195.1

Appendix TABLE VIII
DETAILED CONSTITUENT COST DATA FOR A 1.4 GW VSC–HVDC SYSTEM

HVDC		Transmission Distance l (km)												
		0	20	40	60	80	100	120	140	160	180	200	220	240
Cost (M£)	*TCC*	292	292	292	292	292	292	292	292	292	292	292	292	292
	TLC	74.4	74.3	74.3	74.3	74.2	74.2	74.2	74.1	74.1	74.1	74.0	74.0	74.0
	RCC	0	23.5	47.0	70.5	94.0	117.5	141.0	164.5	188.0	211.5	235.0	258.5	282.0
	RLC	0	3.7	7.4	11.0	14.7	18.4	22.1	25.7	29.4	33.1	36.8	40.4	44.1
	C	366.4	393.5	420.7	447.8	474.9	502.1	529.3	556.3	583.5	610.7	637.8	664.9	692.1

Appendix TABLE IX
DETAILED CONSTITUENT COST DATA FOR A 1.4 GW LFAC SYSTEM

LFAC		Transmission Distance l (km)												
		0	20	40	60	80	100	120	140	160	180	200	220	240
Cost (M£)	*TCC*	201.4	201.4	201.4	201.4	201.4	201.4	201.4	201.4	201.4	201.4	201.4	201.4	201.4
	TLC	33.3	33.2	33.2	33.2	33.1	33.1	33.1	33.0	33.0	33.0	33.0	33.0	33.0
	RCC	0	57.7	115.5	173.2	231.0	288.7	346.5	404.2	461.9	519.7	577.4	702.6	766.5
	RLC	0	3.8	7.7	11.5	15.3	19.1	23.0	26.8	30.6	34.4	38.3	35.4	38.6
	C	231.7	293.1	354.8	416.3	477.8	539.3	601.0	662.4	723.9	785.5	847.0	969.4	1036.2

Appendix TABLE X
PARAMETERS OF THE TYPICAL OHL IN A HVAC SYSTEM

Nominal Voltage V_{n} (kV)	380	500	750
OHL type	562-AL1/49-ST1A	494-AL1/34-ST1A	653-AL1/45-ST1A
Aluminium area (mm^2)	2 × 562	3 × 494	4 × 653
Nominal current I_{n} (A)	2100	2850	4380
Resistance r_{o} (Ω/km)	0.029	0.022	0.012
Reactance X_{o} (Ω/km)	0.33	0.30	0.29
OHL cost per circuit c_{o} (k£/km)	165	245	370

Appendix TABLE XI
PARAMETERS OF THE TYPICAL OHL IN A CSC–HVDC SYSTEM

Nominal Voltage V_{n} (kV)	± 300	± 400	± 600
OHL type	562-AL1/49-ST1A	494-AL1/34-ST1A	653-AL1/45-ST1A
Aluminium area (mm^2)	2 × 562	3 × 494	4 × 653
Nominal current I_{n} (A)	2620	3560	5470
OHL cost per circuit c_o (k£/km)	165	245	370

Appendix TABLE XII
PARAMETERS OF THE TYPICAL OHL IN A LFAC SYSTEM

Nominal Voltage V_{n} (kV)	380	500	750
OHL type	562-AL1/49-ST1A	494-AL1/34-ST1A	653-AL1/45-ST1A
Aluminium area (mm^2)	2 × 562	3 × 494	4 × 653
Nominal current I_{n} (A)	2520	3420	5250
Resistance r_{o} (Ω/km)	0.019	0.015	0.0079
Reactance X_{o} (Ω/km)	0.11	0.10	0.097
OHL cost per circuit c_{o} (k£/km)	165	245	370

Appendix TABLE XIII
DETAILED CONSTITUENT COST DATA FOR A 3.0 GW HVAC SYSTEM

HVAC		Transmission Distance l (km)										
		0	150	300	450	600	750	900	1050	1200	1350	1500
Cost (M£)	*TCC*	39.1	39.1	39.1	39.1	39.1	39.1	39.1	39.1	39.1	39.1	39.1
	TLC	55.5	55.2	55.0	54.7	54.5	54.8	54.7	54.6	54.5	54.7	54.6
	RCC	0	55.5	111	166.5	222	555	666	777	888	1498.5	1665
	RLC	0	43.3	86.5	129.8	173.0	108.1	129.8	151.4	173.0	129.8	144.2
	C	92.6	191.1	289.6	388.1	486.6	755.0	887.6	1020.1	1152.6	1720.4	1900.9

Appendix TABLE XIV
DETAILED CONSTITUENT COST DATA FOR A 3.0 GW CSC–HVDC SYSTEM

HVDC		Transmission Distance l (km)										
		0	150	300	450	600	750	900	1050	1200	1350	1500
Cost (M£)	*TCC*	354	354	354	354	354	354	354	354	354	354	354
	TLC	79.4	79.4	79.3	79.2	79.1	79.0	78.9	78.8	78.7	78.6	78.5
	RCC	0	37.5	75	112.5	150	187.5	225	262.5	300	337.5	375
	RLC	0	21.2	42.4	63.6	84.8	106.0	127.3	148.5	169.7	190.9	212.1
	C	433.4	492.1	550.7	609.3	667.9	726.5	785.1	843.8	902.4	961.0	1019.6

Appendix TABLE XV
DETAILED CONSTITUENT COST DATA FOR A 3.0 GW LFAC SYSTEM

LFAC		Transmission Distance l (km)										
		0	150	300	450	600	750	900	1050	1200	1350	1500
Cost (M£)	*TCC*	209.0	209.0	209.0	209.0	209.0	209.0	209.0	209.0	209.0	209.0	209.0
	TLC	65.0	64.8	64.5	64.3	64.0	64.8	64.5	64.3	64.0	63.8	63.5
	RCC	0	55.5	111	166.5	222	277.5	333	388.5	444	499.5	555
	RLC	0	28.4	56.9	85.3	113.8	142.2	170.6	199.1	227.5	255.9	284.4
	C	277.0	360.7	444.4	528.1	611.8	695.5	779.1	862.9	946.5	1030.2	1113.9

Appendix TABLE XVI
DETAILED CONSTITUENT COST DATA FOR A 5.0 GW HVAC SYSTEM

HVAC		Transmission Distance l (km)										
		0	150	300	450	600	750	900	1050	1200	1350	1500
Cost (M£)	*TCC*	55.7	55.7	55.7	55.7	55.7	55.7	55.7	55.7	55.7	55.7	55.7
	TLC	88.8	88.5	88.1	87.7	87.4	87.0	87.4	87.1	87.4	87.2	87.0
	RCC	0	111	222	333	444	555	999	1165.5	1776	1998	2220
	RLC	0	60.1	120.1	180.2	240.3	300.4	240.3	280.3	240.3	270.3	300.4
	C	146.7	317.4	488.1	658.8	829.6	1000.3	1384.6	1590.9	2161.6	2413.4	2665.3

Appendix TABLE XVII
DETAILED CONSTITUENT COST DATA FOR A 5.0 GW CSC–HVDC SYSTEM

HVDC		Transmission Distance l (km)										
		0	150	300	450	600	750	900	1050	1200	1350	1500
Cost (M£)	*TCC*	590	590	590	590	590	590	590	590	590	590	590
	TLC	132.4	132.2	131.9	131.6	131.4	131.1	130.9	130.6	130.4	130.1	129.8
	RCC	0	37.5	75	112.5	150	187.5	225	262.5	300	337.5	375
	RLC	0	58.9	117.8	176.7	235.7	294.6	353.5	412.4	471.3	530.2	589.1
	C	722.4	818.6	914.7	1010.9	1107.0	1203.2	1299.3	1395.5	1491.7	1587.8	1684.0

Appendix TABLE XVIII
DETAILED CONSTITUENT COST DATA FOR A 5.0 GW LFAC SYSTEM

LFAC		Transmission Distance l (km)										
		0	150	300	450	600	750	900	1050	1200	1350	1500
Cost (M£)	*TCC*	346.7	346.7	346.7	346.7	346.7	346.7	346.7	346.7	346.7	346.7	346.7
	TLC	115.7	115.0	114.2	113.5	112.8	112.1	111.3	110.6	112.8	112.4	112.1
	RCC	0	55.5	111	166.5	222	277.5	333	388.5	888	999	1110
	RLC	0	83.3	166.7	250.0	333.4	416.7	500.0	583.4	333.4	375.0	416.7
	C	455.1	593.2	731.3	869.4	1007.6	1145.7	1283.7	1422.0	1673.6	1825.8	1978.2

REFERENCES

[1] Energy Information Administration. (2017, Sep.). International energy outlook 2017. [Online]. Available: https://www.eia.gov/outlooks/ieo/pdf/0484(2017).pdf.

[2] X. C. Zhang, C. Ma, X. Song, Y. Y. Zhou, and W. P. Chen, "The impacts of wind technology advancement on future global energy," *Applied Energy*, vol. 184, pp. 1033–1037, Dec. 2016.

[3] Eurostat. (2021, Feb.). Share of renewable energy in gross final energy consumption. [Online]. Available: https://ec.europa.eu/eurostat/tgm/refreshTableAction.do?tab=table&plugin=1&pcode=sdg_07_40&language=en.

[4] U. S. Department of Energy. (2018). 2018 Wind Technologies Market Report, [Online]. Available: https://www.energy.gov/sites/prod/files/2019/08/f65/2018%20Wind%20Technologies%20Market%20Report%20FINAL.pdf.

[5] T. Ackermann, *Wind Power in Power Systems*, 2nd ed., Chichester, UK: Wiley, 2012.

[6] J. Feng and W. Z. Shen, "Design optimization of offshore wind farms with multiple types of wind turbines," *Applied Energy*, vol. 205, pp. 1283–1297, Nov. 2017.

[7] Wind Europe. (2019, Feb.). Offshore wind in Europe. [Online]. Available: https://windeurope.org/wp-content/uploads/files/about-wind/statistics/WindEurope-Annual-Offshore-Statistics-2018.pdf.

[8] P. Ark. (2009, Aug.). China starts building first 10-GW mega wind farm. [Online]. Available: https://www.reuters.com/article/us-china-wind-power/china-starts-building-first-10-gw-mega-wind-farm-idUSTRE5771IP20090808.

[9] M. Liserre, R. Cárdenas, M. Molinas, and J. Rodriguez, "Overview of multi-MW wind turbines and wind parks," *IEEE Transactions on Industrial Electronics*, vol. 58, no. 4, pp. 1081–1095, Apr. 2011.

[10] T. Conlon, M. Waite, and V. Modi, "Assessing new transmission and energy storage in achieving increasing renewable generation targets in a regional grid," *Applied Energy*, vol. 250, pp. 1085–1098, Sep. 2019.

[11] M. Aredes, R. Dias, A. F. Da Cunha De Aquino, C. Portela and E. Watanabe, "Going the distance," *IEEE Industrial Electronics Magazine*, vol. 5, no. 1, pp. 36–48, Mar. 2011.

[12] S. Cole and R. Belmans, "Transmission of bulk power," *IEEE Industrial Electronics Magazine*, vol. 3, no. 3, pp. 19–24, Sep. 2009.

[13] S. Rao, *EHV-Ac, Hvdc Transmission & Distribution Engineering*, 3rd ed. Khanna Publishers, 2013.

[14] K. Hafeez and S. A. Khan, "High voltage direct current (HVDC) transmission: Future expectation for Pakistan," *CSEE Journal of Power and Energy Systems*, vol. 5, no. 1, pp. 82–86, March 2019.

[15] L. P. Lazaridis, "Economic comparison of HVAC and HVDC solutions

for large offshore wind farms under special consideration of reliability, " M. S. thesis, Department, Royal Institute of Technology, Stockholm, 2005.

[16] M. I. Blanco, "The economics of wind energy," *Renewable and Sustainable Energy Reviews*, vol. 13, no. 6–7, pp. 1372–1382, Aug. /Sep. 2009.

[17] B. Van Eeckhout, D. Van Hertem, M. Reza, K. Srivastava, and R. Belmans, "Economic comparison of VSC HVDC and HVAC as transmission system for a 300 MW offshore wind farm, " *European Transactions on Electrical Power*, vol. 20, no. 5, pp. 667–671, Jul. 2010.

[18] A. Madariaga, I. Martínez de Alegría, J. L. Martín, P. Eguía, and S. Ceballos, "Current facts about offshore wind farms," *Renewable and Sustainable Energy Reviews*, vol. 16, no. 5, pp. 3105–3116, Jun. 2012.

[19] M. P. Bahrman and B. K. Johnson, "The ABCs of HVDC transmission technologies," *IEEE Power and Energy Magazine*, vol. 5, no. 2, pp. 32–44, Mar./Apr. 2007.

[20] D. Van Hertem and M. Ghandhari, "Multi-terminal VSC HVDC for the European supergrid: obstacles," *Renewable and Sustainable Energy Reviews*, vol. 14, no. 9, pp. 3156–3163, Dec. 2010.

[21] D. Elliott, K. R. W. Bell, S. J. Finney, R. Adapa, C. Brozio, J. Yu, and K. Hussain, "A comparison of AC and HVDC options for the connection of offshore wind generation in great Britain," *IEEE Transactions on Power Delivery*, vol. 31, no. 2, pp. 798–809, Apr. 2016.

[22] J. Arrillaga, Y. H. Liu, and N. R. Watson, *Flexible Power Transmission: The HVDC Options*, Chichester, UK: John Wiley and Sons, 2007.

[23] Alstom Grid, *HVDC: Connecting to the Future*, Alstom Publishers, 2010.

[24] Ørsted. (2019, Jun.). Hornsea One. [Online]. Available: https://hornseaprojectone.co.uk/.

[25] Ørsted. (2018, Oct.). Hornsea project one-project overview: presentation for Ofgem OFTO. [Online]. Available: https://www.ofgem.gov.uk/system/files/docs/2018/10/hornsea_one_project_presentation.pdf.

[26] SSE. Dogger Bank Wind Farms. [Online]. Available: https://doggerbank.com/.

[27] SSE. The project at a glance. [Online]. Available: https://doggerbank.com/downloads/3-Dogger-Bank-at-a-glance.pdf.

[28] T. Funaki and K. Matsuura, "Feasibility of the low frequency AC transmission," in *IEEE PES Winter Meeting*, Singapore, 2000, pp. 2693–2698.

[29] J. Ruddy, R. Meere, and T. O'Donnell, "Low Frequency AC transmission for offshore wind power: A review," *Renewable and Sustainable Energy Reviews*, vol. 56, pp. 75–86, Apr. 2016.

[30] I. Erlich, F. Shewarega, H. Wrede, and W. Fischer, "Low frequency AC for offshore wind power transmission-prospects and challenges," in *11th IET International Conference on AC and DC Power Transmission*, Birmingham, Feb. 2015, pp. 1–7.

[31] X. F. Wang and X. L. Wang, "Feasibility study of fractional frequency transmission system," *IEEE Transactions on Power Systems*, vol. 11, no. 2, pp. 962–967, May 1996.

[32] J. Li and X. P. Zhang, "Small signal stability of fractional frequency transmission system with offshore wind farms," *IEEE Transactions on Sustainable Energy*, vol. 7, no. 4, pp. 1538–1546, Oct. 2016.

[33] S. Q. Liu, X. F. Wang, L. H. Ning, B. Y. Wang, M. Lu, and C. C. Shao, "Integrating offshore wind power via fractional frequency transmission system," *IEEE Transactions on Power Delivery*, vol. 32, no. 3, pp. 1253–1261, Jun. 2017.

[34] S. Chaithanya, V. N. B. Reddy, and R. Kiranmayi, "A state of art review on offshore wind power transmission using low frequency AC system," *International Journal of Renewable Energy Research*, vol. 8, no. 1, 141–149, Mar. 2018.

[35] T. Ngo, M. Lwin, and S. Santoso, "Steady-state analysis and performance of low frequency AC transmission lines," *IEEE Transactions on Power Systems*, vol. 31, no. 5, pp. 3873–3880, Sep. 2016.

[36] J. Ruddy, R. Meere, C. O'Loughlin, and T. O'Donnell, "Design of VSC connected low frequency AC offshore transmission with long HVAC cables," *IEEE Transactions on Power Delivery*, vol. 33, no. 2, pp. 960–970, Apr. 2018.

[37] H. Chen, M. H. Johnson, and D. C. Aliprantis, "Low-frequency AC transmission for offshore wind power," *IEEE Transactions on Power Delivery*, vol. 28, no. 4, pp. 2236–2244, Oct. 2013.

[38] S. Q. Liu, X. F. Wang, Y. Q. Meng, P. W. Sun, H. Y. Luo, and B. Y. Wang, "A decoupled control strategy of modular multilevel matrix converter for fractional frequency transmission system," *IEEE Transactions on Power Delivery*, vol. 32, no. 4, pp. 2111–2121, Aug. 2017.

[39] X. F. Wang, C. J. Cao, and Z. C. Zhou, "Experiment on fractional frequency transmission system," *IEEE Transactions on Power Systems*, vol. 21, no. 1, pp. 372–377, Feb. 2006.

[40] X. F. Wang, X. H. Wei, and Y. Q. Meng, "Experiment on grid-connection process of wind turbines in fractional frequency wind power system," *IEEE Transactions on Energy Conversion*, vol. 30, no. 1, pp. 22–31, Mar. 2015.

[41] M. de Prada Gil, O. Gomis-Bellmunt, and A. Sumper, "Technical and economic assessment of offshore wind power plants based on variable frequency operation of clusters with a single power converter," *Applied Energy*, vol. 125, pp. 218–229, Jul. 2014.

[42] X. F. Wang, Y. F. Teng, L. H. Ning, Y. Q. Meng, and Z. Xu, "Feasibility of integrating large wind farm via Fractional Frequency Transmission System a case study," *International Transactions on Electrical Energy Systems*, vol. 24, no. 1, pp. 64–74, Jan. 2014.

[43] S. Meliopoulos, D. Aliprantis, Y. Cho, D. Zhao, A. Keeli, and H. Chen, "Low Frequency Transmission," [Online]. Available: https://pserc.wisc.edu/documents/publications/reports/2012_reports/S-42_Final-Report_Nov-2012.pdf.

[44] X. Xiang, M. M. C. Merlin, and T. C. Green, "Cost analysis and comparison of HVAC, LFAC and HVDC for offshore wind power connection," in *12th IET International Conference on AC and DC Power Transmission (ACDC 2016)*, Beijing, 2016, pp. 1–6.

[45] S. Hardy, K. Van Brusselen, S. Hendrix, D. Van Hertem, and H. Ergun, "Techno-economic analysis of HVAC, HVDC and OFAC offshore wind power connections," in *2019 IEEE Milan PowerTech*, Milan, Italy, 2019, pp. 1–6.

[46] J. L. Domínguez-García, D. J. Rogers, C. E. Ugalde-Loo, J. Liang, and O. Gomis-Bellmunt, "Effect of non-standard operating frequencies on the economic cost of offshore AC networks," *Renewable Energy*, vol. 44, pp. 267–280, Aug. 2012.

[47] N. Qin, S. You, Z. Xu, and V. Akhmatov, "Offshore wind farm connection with low frequency AC transmission technology," in *IEEE PES General Meeting*, Calgary, AB, 2009, pp. 1–8.

[48] S. Karamitsos, A. Canelhas, U. Axelsson, and E. Olsen, "Low frequency AC transmission on large scale offshore wind power plants–achieving the best from two worlds?" in *13th Wind Integration Workshop*, Berlin, 2014, pp. 1–7.

[49] P. Bresesti, W. L. Kling, R. L. Hendriks, and R. Vailati, "HVDC connection of offshore wind farms to the transmission system," *IEEE Transactions on Energy Conversion*, vol. 22, no. 1, pp. 37–43, Mar. 2007.

[50] B. Snyder and M. Kaiser, "Ecological and economic cost-benefit analysis of offshore wind energy," *Renewable Energy*, vol. 34, no. 6, pp. 1567–1578, Jun. 2009.

[51] M. Dicorato, G. Forte, M. Pisani, and M. Trovato, "Guidelines for assessment of investment cost for offshore wind generation," *Renewable Energy*, vol. 36, no. 8, pp. 2043–2051, Aug. 2011.

[52] S. Lauria, M. Schembari, F. Palone, and M. Maccioni, "Very long distance connection of gigawatt-size offshore wind farms: extra high-voltage AC versus high-voltage DC cost comparison," *IET Renewable Power Generation*, vol. 10, no. 5, pp. 713–720, May 2016.

[53] D. Schoenmakers, "Optimization of the coupled grid connection of offshore wind farms, " M. S. thesis, Department, Technical University of Eindhoven, Raamsdonksveer, Sep. 2008.

[54] P. Djapic and G. Strbac, "Cost benefit methodology for optimal design of offshore transmission systems," in *Department for Business, Enterprise & Regulatory Reform*, 2009.

[55] S. Rodrigues, C. Restrepo, E. Kontos, R. Pinto, and P. Bauer, "Trends of offshore wind projects," *Renewable and Sustainable Energy Reviews*, vol. 49, pp. 1114–1135, Jun. 2015.

[56] National Grid, "Electricity ten year statement, appendix E–technology," *UK Electricity Transmission*, Nov. 2015.

[57] N. B. Negra, J. Todorovic, and T. Ackermann, "Loss evaluation of HVAC and HVDC transmission solutions for large offshore wind farms," *Electric Power Systems Research*, vol. 76, no. 11, pp. 916–927, Jul. 2006.

[58] B. Van Eeckhout, "The economic value of VSC HVDC compared to HVAC for offshore wind farms," M. S. thesis, Department, K. U. Leuven, Belgium, Oct. 2008.

[59] I. Martínez de Alegría, J. L. Martín, I. Kortabarria, J. Andreu, and P. Ibañez-Ereño, "Transmission alternatives for offshore electrical power," *Renewable and Sustainable Energy Reviews*, vol. 13, no. 5, pp. 1027–1038, Jun. 2009.

[60] J. De Decker and A. Woyte, "Review of the various proposals for the European offshore grid," *Renewable Energy*, vol. 49, pp. 58–62, Jan. 2013.

[61] National Grid, "Electricity Ten Year Statement, Appendix H–Transmission Losses," *UK Electricity Transmission*, Nov. 2015.

[62] T. Ackermann, N. Negra, J. Todorovic, and L. Lazaridis, "Evaluation of electrical transmission concepts for large offshore wind farms," in *Copenhagen Offshore Wind Conference and Exhibition*, Copenhagen, pp. 1–10, 2005.

[63] J. Song-Manguelle, T. M. Harfman, S. Chi, S. K. Gunturi, and R. Datta, "Power transfer capability of HVAC cables for subsea transmission and distribution systems," in *60th Annual Petroleum and Chemical Industry Conference*, Chicago, IL, 2013, pp. 1–9.

[64] P. B. Wyllie, Y. Tang, L. Ran, T. Yang, and J. Yu, "Low frequency AC transmission-elements of a design for wind farm connection," in

11th IET International Conference on AC and DC power transmission, Birmingham, 2015, pp. 1–5.
[65] M. A. Hannan, M. S. H. Lipu, P. J. Ker, R. A. Begum, V. G. Agelidis, and F. Blaabjerg, "Power electronics contribution to renewable energy conversion addressing emission reduction: Applications, issues, and recommendations," *Applied Energy*, vol. 251, pp. 113404, Oct. 2019.
[66] K. W. Lao, Q. Nguyen, and S. Santoso, "Power electronic converters for low-frequency HVac transmission: functions and challenges," in *2018 IEEE Power & Energy Society General Meeting*, Portland, OR, 2018, pp. 1–5.
[67] R. Nakagawa, T. Funaki, and K. Matsuura, "Installation and control of cycloconverter to low frequency AC power cable transmission," in *Proceedings of the Power Conversion Conference-Osaka 2002*, Osaka, Japan, vol. 3, pp. 1417–1422, 2002.
[68] Y. Cho, G. J. Cokkinides, and A. P. Meliopoulos, "Time domain simulation of a three-phase cycloconverter for LFAC transmission systems," in *IEEE PES Transmission and Distribution Conference and Exhibition*, Orlando, FL, 2012, pp. 1–8.
[69] Y. Cho, G. J. Cokkinides, and A. P. Meliopoulos, "LFAC-transmission systems for remote wind farms using a three-phase, six-pulse cycloconverter," in *2012 IEEE Power Electronics and Machines in Wind Applications*, Denver, CO, 2012, pp. 1–7.
[70] P. Achara and T. Ise, "Power control of low frequency AC transmission system using cycloconverters with virtual synchronous generator control," in *41st Annual Conference of the IEEE Industrial Electronics Society*, Yokohama, 2015, pp. 2661–2666.
[71] Y. Tang, P. B. Wyllie, J. Yu, X. M. Wang, L. Ran, and O. Alatise, "Offshore low frequency AC transmission with back-to-back modular multilevel converter (MMC)," in *11th IET International Conference on AC and DC Power Transmission*, Birmingham, 2015, pp. 1–8.
[72] T. Lüth, M. M. C. Merlin, T. C. Green, F. Hassan, and C. Barker, "High-frequency Operation of a DC/AC/DC System for HVDC Applications," *IEEE Transactions on Power Electronics*, vol. 29, no. 8, pp. 4107–4115, Aug. 2014.
[73] H. Akagi, "Classification, terminology, and application of the modular multilevel cascade converter (MMCC)," *IEEE Transactions on Power Electronics*, vol. 26, no. 11, pp. 3119–3130, Nov. 2011.
[74] Y. Miura, T. Mizutani, M. Ito, and T. Ise, "Modular multilevel matrix converter for low frequency AC transmission," in *2013 IEEE 10th International Conference on Power Electronics and Drive Systems*, Kitakyushu, 2013, pp. 1079–1084.
[75] S. Q. Liu, M. Saeedifard, and X. F. Wang, "Analysis and control of the modular multilevel matrix converter under unbalanced grid conditions," *IEEE Journal of Emerging and Selected Topics in Power Electronics*, vol. 6, no. 4, pp. 1979–1989, Dec. 2018.
[76] C. A. S. Rangel and F. Mancillan-David, "Hexverter-based optimal low frequency AC transmission system," in *2018 North American Power Symposium*, Fargo, ND, 2018, pp. 1–5.
[77] P. W. Sun, X. F. Wang, L. H. Ning, S. Q. Liu, L. Tang, and M. Lu, "The application of modular multilevel matrix converter in fractional frequency offshore wind power system," in *16th International Conference on Environment and Electrical Engineering*, Florence, 2016, pp. 1–4.
[78] G. Stamatiou, "Techno-economical analysis of DC collection grid for offshore wind parks, " M. S. thesis, Department, The University of Nottingham, Nottingham, 2010.
[79] Siemens. High-performance power highways with HVDC Classic. [Online]. Available: https://new.siemens.com/global/en/products/energy/high-voltage/high-voltage-direct-current-transmission-solutions/hvdc-classic.html.
[80] W. Fischer, R. Braun, and I. Erlich, "Low frequency high voltage offshore grid for transmission of renewable power," in *3rd IEEE PES Innovative Smart Grid Technologies Europe*, Berlin, 2012, pp. 1–6.
[81] A. Canelhas, S. Karamitsos, U. Axelsson, and E. Olsen, "A low frequency power collector alternative system for long cable offshore wind generation," in *11th IET International Conference on AC and DC Power Transmission*, Birmingham, 2015, pp. 1–6.
[82] D. N. Kossyvakis, A. I. Chrysochos, and K. Pavlou, "Calculation of losses in three-core submarine cables for fractional frequency transmission operation," in *IEEE International Conference on High Voltage Engineering and Application*, Athens, Greece, 2018, pp. 1–4.
[83] ABB. HVDC References. [Online]. Available: https://new.abb.com/systems/hvdc/references.
[84] Siemens. HVDC-high voltage direct current transmission. [Online]. Available: https://w3.siemens.com.br/topics/br/pt/EM/Documents/Infografico_Siemens_SNPTEE/pdfs/hvdc/hvdc002_HVDC_References.pdf
[85] GE Grid Solutions. High voltage direct current systems. [Online]. Available: https://www.gegridsolutions.com/products/brochures/ powerd_vtf/HVDC-Systems_GEA-31971_LR.pdf.
[86] ENTSO-e. (2018). TYNDP 2018 projects sheets. [Online]. Available: https://tyndp.entsoe.eu/tyndp2018/projects/projects.
[87] Global Transmission Research, "Cross-border and Interconnector Projects Database and Report," *Technical Report*, Sep. 2017.
[88] Asso Group. (2014). Capri-torre annunziata interconnection. [Online]. Available: http://www. assogroup. com/en/projects/2014/capri-torre-annunziata-interconnection/
[89] Terna Group. Terna meets Sorrento. [Online]. Available: https://www.terna.it/en/projects/public-engagement/terna-meets-sorrento.
[90] 50Hertz Transmission GmbH. Kriegers Flak–combined grid solution. [Online]. Available: https://www.50hertz.com/en/Grid/Griddevelopement/Offshoreprojects/CombinedGridSolution.
[91] Energinet. Kriegers flak–combined grid solution. [Online].Available: https://en.energinet.dk/Infrastructure-Projects/Projektliste/KriegersFlak CGS.
[92] ElecLink. What we do. [Online]. Available: http://www.eleclink.co.uk/index.php.
[93] Getlink Group. A 1GW electrical interconnector between the United Kingdom and France via the Channel Tunnel. [Online]. Available: https://www.getlinkgroup.com/uk/group/eleclink/.
[94] ENTSO-e. Project 179-DKE-DE (Kontek2). [Online]. Available: https://tynd-p.entsoe.eu/tyndp2018/projects/projects/179.
[95] Energy Reporters. (2019, May). Italy and Tunisia agree 600MW interconnector. [Online]. Available: https://www.energy-reporters.com/transmission/italy-and-tunisia-agree-600mw-interconnector-deal/.
[96] F. Kiessling, P. Nefzger, J. F. Nolasco, and U. Kaintzyk, *Overhead Power Lines, Planning Design Construction*, Berlin, Heidelberg, New York: Springer Publishers, 2003.
[97] B. S. Mohan, C. B. Shankaralingappa, and R. Prakash, "Fractional frequency transmission system to enhance line loadability in EHVAC & UHVAC long transmission line," in *2014 International Conference on Advances in Electronics Computers and Communications*, Bangalore, 2014, pp. 1–6.

Xin Xiang (S'17–M'18) received the B.Sc. degree from Harbin Institute of Technology, China in 2011, the M.Sc. degree from Zhejiang University, China in 2014 and the Ph.D. degree from Imperial College London, UK in 2018, all in Electrical and Electronic Engineering. He has received the Eryl Cadwaladr Davies Prize for the Best Ph.D. Thesis of the Electrical and Electronic Engineering Department in the Imperial College London, and he was also the recipient of the Best Ph.D. Thesis Award from IEEE PELS UK and Ireland Chapter. From 2018 to 2020, he was a Research Associate with the Imperial College London, UK. He is currently a tenure-track Associate Professor in the College of Electrical Engineering, Zhejiang University, China. His research interests include the analysis and control of power electronics converters for power system applications.

Shiyuan Fan received the B.Sc. degree in Electrical Engineering and its Automation from North China Electric Power University, Beijing, China, in 2018. She is currently working toward the Ph.D. degree in Electrical Engineering at Zhejiang University, Zhejiang, China.

Her research interests include control of modular multilevel converters.

Yunjie Gu (M'16–SM'20) received the B.Sc. and the Ph.D. degrees in Electrical Engineering from Zhejiang University, Hangzhou, China, in 2010 and 2015 respectively. He was a Consulting Engineer with General Electric Global Research Centre, Shanghai, China, from 2015 to 2016. After that, he joined the Imperial College, UK, under the sponsorship of the UKRI Innovation Fellowship. He is currently a Lecturer (Assistant Professor) with the University of Bath, UK, and an Honorary Lecturer at the Imperial College. His research focuses on the fundamental theories and computational tools for analyzing power system dynamics, as well as the algorithms and software for power conversion control.

Wenlong Ming (M'17) received the B. Eng. and M. Eng. degrees in Automation from Shandong University, Jinan, China, in 2007 and 2010, respectively, and the Ph.D. degree in Automatic Control and Systems Engineering from the University of Sheffield, Sheffield, U.K., in 2015.

He has been a Lecturer of Power Electronics with Cardiff University, Cardiff, U. K., since 2016, and a Senior Research Fellow funded by Compound Semiconductor Applications, Catapult, U.K., for 5 years, since 2020. His current research interests include medium-voltage dc systems for electricity distribution networks and characterization, modeling, and applications of wide-bandgap compound semiconductors.

Dr. Ming was the winner of the prestigious IET Control & Automation Doctoral Dissertation Prize in 2017.

Jianzhong Wu (M'14) received the B.S., M.S., and Ph.D. degrees in electrical engineering from Tianjin University, Tianjin, China, in 1999, 2002, and 2004, respectively. He is currently a Professor of Multivector Energy Systems and the Head of the School of Engineering, Cardiff University, Cardiff, U.K. His current research interests include energy infrastructure and smart grids.

Prof. Wu is an Associate Editor for Applied Energy. He is a Co-Director of UK Energy Research Center and EPSRC Supergen Hub on Energy Networks.

Wuhua Li (M'09) received the B.Sc. and Ph.D. degrees in Power Electronics and Electrical Engineering from Zhejiang University, Hangzhou, China, in 2002 and 2008, respectively.

From 2004 to 2005, he was a Research Intern, and from 2007 to 2008, a Research Assistant in the GE Global Research Center, Shanghai, China. From 2008 to 2010, he joined the College of Electrical Engineering, Zhejiang University as a Post doctor. In 2010, he was promoted to an Associate Professor. Since 2013, he has been a Full Professor at Zhejiang University. From 2010 to 2011, he was a Ryerson University Postdoctoral Fellow with the Department of Electrical and Computer Engineering, Ryerson University, Toronto, ON, Canada. He is currently the Executive Deputy Director of the National Specialty Laboratory for Power Electronics and the Vice Director of the Power Electronics Research Institute, Zhejiang University. His research interests include power devices, converter topologies and advanced controls for high power energy conversion systems. Dr. Li has published more than 300 peer-reviewed technical papers and holds over 50 issued/pending patents.

Due to his excellent teaching and research contributions, Dr. Li received the 2012 Delta Young Scholar from Delta Environmental & Educational Foundation, 2012 Outstanding Young Scholar from National Science Foundation of China (NSFC), 2013 Chief Youth Scientist of National 973 Program, 2019 Distinguished Young Scholar from National Science Foundation of China. He serves as the Associate Editor of the Journal of Emerging and Selected Topics in Power Electronics, IET Power Electronics, CSEE Journal of Power and Energy Systems, CPSS Transactions on Power Electronics and Applications, Proceedings of the Chinese Society for Electrical Engineering, Guest Editor of IET Renewable Power Generation for Special Issue "DC and HVDC system technologies," Member of Editorial Board for Journal of Modern Power System and Clean Energy.

He received one National Natural Science Award and four Scientific and Technological Achievement Awards from Zhejiang Provincial Government and the State Educational Ministry of China. He was appointed as one of the Most Cited Chinese Researchers by Elsevier since 2014.

Xiangning He (M'95–SM'96–F'10) received the B.Sc. and M.Sc. degrees from Nanjing University of Aeronautical and Astronautical, Nanjing, China, in 1982 and 1985, respectively, and the Ph.D. degree from Zhejiang University, Hangzhou, China, in 1989. From 1985 to 1986, he was an Assistant Engineer at the 608 Institute of Aeronautical Industrial General Company, Zhuzhou, China. From 1989 to 1991, he was a Lecturer at Zhejiang University. In 1991, he obtained a Fellowship from the Royal Society of U.K., and conducted research in the Department of Computing and Electrical Engineering, Heriot-Watt University, Edinburgh, U.K., as a Post-Doctoral Research Fellow for two years. In 1994, he joined Zhejiang University as an Associate Professor. Since 1996, he has been a Full Professor in the College of Electrical Engineering, Zhejiang University. He was the Director of the Power Electronics Research Institute, the Head of the Department of Applied Electronics, the Vice Dean of the College of Electrical Engineering, and he is currently the Director of the National Specialty Laboratory for Power Electronics, Zhejiang University. His research interests are power electronics and their industrial applications.

Dr. He is a Fellow of The Institute of Electrical and Electronics Engineers (IEEE) and was appointed as IEEE Distinguished Lecturer by the IEEE Power Electronics Society 2011–2015. He is also a Fellow of the Institution of Engineering and Technology (formerly IEE), U.K.

Timothy. C. Green (M'89–SM'02–F'19) received a B.Sc. (Eng) (first class honors) from the Imperial College London, UK in 1986 and a Ph.D. from Heriot-Watt University, Edinburgh, UK in 1990. He is a Professor of Electrical Power Engineering at Imperial College London, and Director of the Energy Futures Lab with a role of fostering interdisciplinary energy research across the university. His research is focused on using the flexibility of power electronics to further the decarbonization of electricity systems by easing the integrations of renewable sources and EV charging. In HVDC, he has contributed converter designs that strike improved trade-offs between power losses, physical size and fault handling. In distribution systems, he has pioneered the use of soft open points and the study of stability of grid connected inverters. Prof. Green is a Chartered Engineer in the UK and a Fellow of the Royal Academy of Engineering.